Clinical Hyperpolarized ^{129}Xe MRI: Past, Present, and Future

Bastiaan Driehuys
bastiaan.driehuys@duke.edu
Duke University Medical Center, Durham NC

Introduction: MRI using hyperpolarized noble gases was introduced in 1994, and while showing extraordinary promise, has experienced a tortuous clinical development pathway. Athough the elegance of acquiring rapid and non-invasive 3D images of an inhaled, noble gas, captivated many scientists and clinicians from the outset, its widespread clinical dissemination has been slower than might have been expected. Some of the impediment was readily attributed to barriers associated with intellectual property rights, poor corporate stewardship, and a challenging regulatory environment. Fortunately, these issues have now largely been addressed. A second major obstacle was that while ^{129}Xe MRI was always recognized to be the "future", it was ^{3}He with its more mature polarization technology and large gyromagnetic ratio that received the bulk of the clinical development energies for the first decade or so. Although, this provided a superb clinical foundation for the field, it was only the severe ^{3}He supply and price crisis that made it clear that ^{129}Xe development could no longer be postponed. This required overcoming a rather low gyromagnetic ratio, improving both ^{129}Xe polarization and production rate, and paying far more careful attention to optimizing scanner performance for a this nucleus.

These efforts, driven by a large, interdisciplinary community of scientists, engineers and clinicians have now been rewarded. Not only has ^{129}Xe MRI demonstrated the ability to replace ^{3}He for ventilation imaging, but its solubility and chemical shifts have now opened up a far more promising set of opportunities. Specifically, these properties of ^{129}Xe make it uniquely suited to imaging pulmonary gas exchange, the most fundamental function of the lung. ^{129}Xe exhibits distinct resonant frequencies in the airspaces, interstitial barrier and red blood cells (RBCs) and, although its instantaneous signal in the latter compartments is relatively tiny (~1-2% of airspace signal), imaging them is enabled by continuous transfer of magnetization from the airspaces. In fact, after a single breath of ^{129}Xe, it is now possible to use an interleaved, short TE, radial acquisition, with phase-based separation of the barrier and RBCs to reveal the ^{129}Xe distribution in each of the three compartments. This approach is now positioning ^{129}Xe MRI to provide a fundamentally new view of pulmonary disease that goes well-beyond ventilatory obstruction. In fact, it is the only way to gain insights into diseases in which ventilation defects are not the primary cause of dyspnea. Specifically, it reveals interstitial thickening, as well as pulmonary vascular occlusions, both of which impair gas exchange. The ability to assess this non-invasively is poised to shed new light on a wide array of disease (figure).

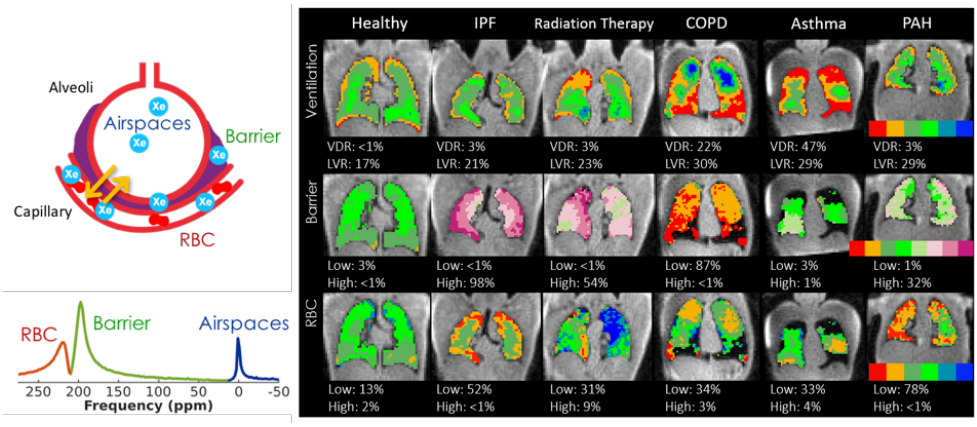

In this talk, I will review the history of hyperpolarized ^{129}Xe development, key clinical and technical milestones, as well as the commercial and regulatory progress. But these advancements alone are not sufficient for physicians to begin ordering ^{129}Xe scans for their patients. For that to happen, the field must demonstrate that ^{129}Xe MRI has clinical value. The field must recognize that it can only provide a clinical benefit to patients if the scan is used to drive decisions to initiate, modify, stop, or withhold treatment. The goal of the talk is to lay out, not only these efforts to drive that routine clinical adoption, but should also provide guidance to the more basic scientists among us who are developing the next generation of ideas. In fact, their pathway for advancement has now been greatly clarified with pending regulatory approval. Nonetheless, the proponents of those new ideas will be provided a realistic picture of the clinical environment into which their technologies must ultimately fit.

Funding: R01HL105643, R01HL126771, HHSN268201700001C

Building a Better Biomarker: Hyperpolarized ^{129}Xe Magnetic Resonance Imaging of Pediatric Cystic Fibrosis

Giles Santyr PhD

Translational Medicine Program, The Hospital for Sick Children
Department of Medical Biophysics
University of Toronto, ON Canada

email (G.E. Santyr): giles.santyr@sickkids.ca

Pediatric respiratory diseases such as cystic fibrosis, asthma, lung injury and bronchopulmonary dysplasia are significant contributors to childhood mortality and can lead to chronic healthcare issues throughout life. Early diagnosis and intervention can substantially reduce morbidity and impact of pediatric lung disease, on the family, society and the economy. There is a compelling clinical need for lung imaging tools that are reproducible and quantitative in order to detect and follow disease progression and measure response to therapeutic interventions, particularly in the pediatric population. Magnetic Resonance Imaging (MRI) may be well suited for imaging the pediatric lung as it is non-invasive and non-ionizing, allowing safe and repeated use. The addition of hyperpolarized (HP) ^{129}Xe gas allows mapping of regional changes in lung function and has been shown to be well-tolerated and reproducible in pediatric populations. Cystic Fibrosis (CF) is a pediatric lung disease that may benefit significantly from novel biomarkers provided by HP ^{129}Xe MRI, particularly the ventilation defect percent (VDP). VDP is a measure of regional airway obstruction associated with mucous plugging, air trapping and other aspects of functional decline (eg. pulmonary exacerbations) associated with CF.

This presentation will focus on the use of HP ^{129}Xe MRI in pediatric CF populations at the Hospital for Sick Children, with a particular emphasis on acquisition and analysis approaches for measuring VDP. Comparison of VDP to conventional pulmonary function tests and the potential role of VDP for monitoring CF treatment will be highlighted.

Hyperpolarised ^{129}Xe MRI – preliminary experience and pathway to clinical application

Madhwesha Rao (Email: m.rao@sheffield.ac.uk), Graham Norquay, Guilhem Collier, Nigel Hoggard, Paul Griffiths, Jim Wild.

POLARIS, Academic unit of Radiology, University of Sheffield, Sheffield, UK.

Background: A major drawback of using contrast-agent based X-ray CT and MRI for brain imaging is that these methods do not provide a direct measure of the regional gas-uptake because the agents do not cross the intact blood brain barrier[1]. In addition, X-ray CT uses ionizing radiation and MR contrast agents have safety issues related to renal[2] and intracranial complications[3]. Arterial spin labelling methods, which are safe, require averaging over several minutes and to-date have had very limited clinical adoption[4]. Thus a method which can directly image brain perfusion and regional gas-uptake, and is also safe for patients is desirable. HP ^{129}Xe can be inhaled, dissolves in the pulmonary blood, transported to the brain, passively crosses the blood brain barrier and dissolves in the extravascular brain tissue. Moreover, it is fully removed from the human body by exhalation. It has been recently shown that it is possible to direct image HP ^{129}Xe in the brain at the concentration achieved following an inhaled dose of 1 L[5]. The purpose of this abstract is to outline preliminary experience from Sheffield with imaging strategies and preliminary clinical studies.

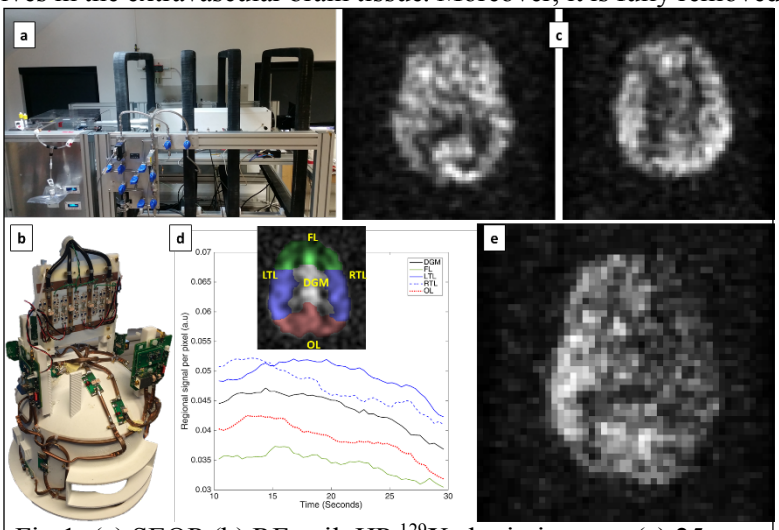

Fig 1: (a) SEOP (b) RF coil. HP ^{129}Xe brain images: (c) 25 mm slice thickness (d) spiral trajectory and (e) stroke subject.

Methods: ^{129}Xe was hyperpolarized (HP) using an in-house SEOP polarizer capable of generating 1 L doses of ^{129}Xe polarized to ~35% in less than 20 minutes[6] (Fig 1a). In-vivo imaging was performed on a 1.5 T GE HDx MRI scanner using a home-built 4 element receiver RF coil array (Fig 1b)[5]. MR imaging was performed with 25 mm slice thickness with all the other parameters as mentioned earlier[5]. A continuous 2D spiral k-space sampling trajectory (TR 400, FA 30°, Δf_0 7.8 kHz, FOV 25) with 16-arm and golden angle up to 64 spirals in total was evaluated for pseudo-temporal dynamic imaging using sliding window reconstruction. A subject (Male 52 years) being monitored from 2 years after a stroke with arterial occlusion and collateralization was imaged with HP ^{129}Xe brain MRI with parameters mentioned earlier[5].

Results: As seen in Fig 1c, the images with 25 mm slice thickness has structural clarity. Fig 1d indicates that the time-resolved spiral trajectory imaging strategy shows regional gas uptake, tissue perfusion and wash-out. Region of lower intensity is seen in the Fig 1e, which indicates region of poor perfusion and gas-uptake, thus demonstrating sensitivity towards pathologies such as intracranial arterial occlusion.

Conclusion: HP ^{129}Xe brain MRI is a safe method which has sensitivity towards brain pathologies related to perfusion, and can also be used for quantitative diagnosis. Evaluating and quantifying the technique in a range of brain pathologies is the scope of future work.

References: 1. Wintermark, M. et al. Stroke 36, e83-99, (2005). 2. Ledneva, E. et al. Rad 250, 618-628 (2009). 3. McDonald, R. J. et al. Rad 275, 772-782 (2015). 4. Alsop, D. C. et al. Mag Res Med 73, 102-116, (2015). 5. Rao, M. R. et al. Rad 0, 162881, doi:10.1148/radiol.2017162881 (2017). 6. Norquay, G. et al. Proc. Intl. Soc. Mag. Reson. Med. 25. P 2140 (2017).

1 Wintermark, M. *et al.* Comparative overview of brain perfusion imaging techniques. *Stroke* **36**, e83-99, doi:10.1161/01.STR.0000177884.72657.8b (2005).
2 Ledneva, E., Karie, S., Launay-Vacher, V., Janus, N. & Deray, G. Renal safety of gadolinium-based contrast media in patients with chronic renal insufficiency. *Radiology* **250**, 618-628, doi:10.1148/radiol.2503080253 (2009).
3 McDonald, R. J. *et al.* Intracranial Gadolinium Deposition after Contrast-enhanced MR Imaging. *Radiology* **275**, 772-782, doi:10.1148/radiol.15150025 (2015).
4 Alsop, D. C. *et al.* Recommended implementation of arterial spin-labeled perfusion MRI for clinical applications: A consensus of the ISMRM perfusion study group and the European consortium for ASL in dementia. *Magnetic Resonance in Medicine* **73**, 102-116, doi:10.1002/mrm.25197 (2015).
5 Rao, M. R., Stewart, N. J., Griffiths, P. D., Norquay, G. & Wild, J. M. Imaging Human Brain Perfusion with Inhaled Hyperpolarized (129)Xe MR Imaging. *Radiology* **0**, 162881, doi:10.1148/radiol.2017162881 (2017).
6 Norquay, G. *et al.* Large-Scale Production of Highly-Polarized 129Xe. *Proc. Intl. Soc. Mag. Reson. Med. 25. P 2140* (2017).

Investigating Regional Pulmonary Gas Transport with Hyperpolarized Xenon-129 Dissolved-Phase MRI

Kai Ruppert[1], Hooman Hamedani[1], Faraz Amzajerdian[1], Luis Loza[1], Yi Xin[1], Tahmina Achekzai[1], Ian F. Duncan[1], Harilla Profka[1], Sarmad Siddiqui[1], Mehrdad Pourfathi[1], Maurizio F. Cereda[2], Stephen Kadlecek[1], Rahim R. Rizi[1]

[1]Department of Radiology, University of Pennsylvania

[2]Department of Anesthesiology, University of Pennsylvania

Email: Kai.Ruppert@uphs.upenn.edu

Background: Existing imaging techniques for detecting lung disorders are unable to measure the degree to which functional impairment of a specific region of the lung contributes to an overall reduction in gas transport. Hyperpolarized xenon-129 (HXe) MRI has previously been used to assess pulmonary gas exchange between the alveolar volume and lung tissue[1-7]. In this work, we quantified changes in the HXe dissolved-phase (DP) signal in response to a regional saturation of the pulmonary gas-phase (GP) signal.

Methods: Imaging experiments were performed in sedated New Zealand rabbits (approx. 4.5 kg). Animals were ventilated with room air until imaging began, at which point the gas mix was switched to 20% oxygen and 80% HXe for two breaths (6 ml/kg tidal volume). Imaging was performed at end inspiration of the second breath. All studies were approved by the Institutional Animal Care and Use Committee.

MR measurements were conducted using either, spectroscopic, 1D or 2D-projection gradient-echo sequences to obtain information about the response of the DP signal following a regional saturation of the GP signal. All MR studies were performed at 1.5T (Avanto; Siemens), using a custom xenon-129 transmit/receive birdcage coil (Stark Contrast, Erlangen, Germany). Enriched xenon gas (87% xenon-129) was polarized using a prototype commercial system (XeBox-E10, Xemed LLC, Durham, NH).

Results: Figure 1 illustrates the principle of the proposed GP saturation technique in the case of a 2D coronal projection acquisition. By destroying the GP magnetization in one region of the lung and subsequently measuring the change in the DP signal in a downstream location such as the heart it can be determined how much the saturated region contributes to the total pulmonary gas transport. Similar implementations for spectroscopic or 1D projection measurements allow the assessment of the gas transport dynamics in the saturated volume at the expense of reduced spatial information.

Conclusion: In this work, we demonstrated how HXe MRI can be used to quantify the contributions of specific lung volumes to overall lung function. These techniques might be especially valuable in lung transplantation, during pharmaceutical interventions, or in the planning of lung-volume reduction surgeries.

Sources of Funding: Supported by NIH grants R01 EB015767 and R01 HL129805.

References: [1] Ruppert et al. NMR Biomed 2000;13:220-228. [2] Driehuys et al. Proc Natl Acad Sci USA 2006;103:18278-18283. [3] Patz et al. Acad Radiol 2008;15:713-727. [4] Mugler et al. Proc Natl Acad Sci USA 2010;107(50):21707-21712. [5] Cleveland et al. Plos One 2010;5:e12192. [6] Qing et al. J Magn Reson Imaging 2013; 39(2):346-359. [7] Doganay et al. Magn Reson Med 2016;76:566-576.

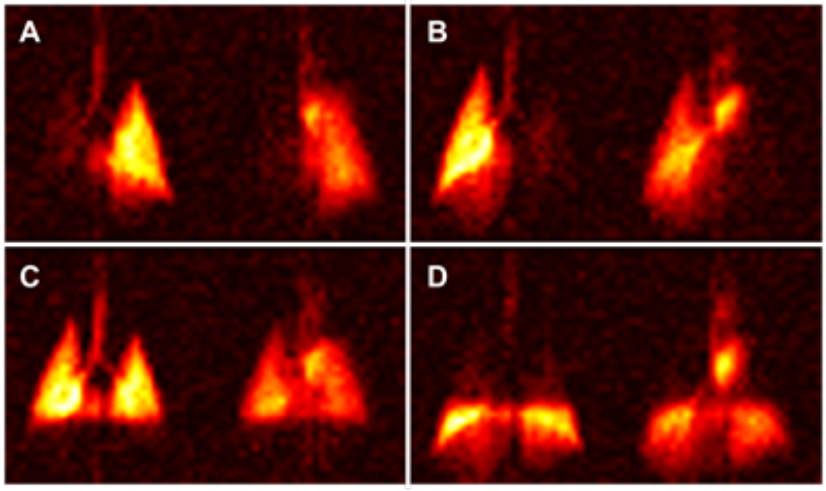

Figure 1. Xenon GP (left side in each panel) and DP (right side in each panel) maps for a flip angle of 40° and a TR of 200 ms following saturation of the GP signal in the (A) right, (B) left, (C) inferior, and (D) superior lung. The signal changes in the DP maps relative to an unsaturated baseline map, in particular in a far downstream location such as the heart, reflect the contributions of the saturated lung volume to total lung function.

Computational studies on xenon NMR

Juha Vaara

NMR Research Unit, P.O. Box 3000, FI-90014 University of Oulu, Finland
juha.vaara@iki.fi

I present a survey of some of the recent computational modelling work on Xe NMR parameters from Oulu, in the topics of

- **spin-exchange optical pumping (SEOP)**: Experimental frequency shifts of ^{129}Xe NMR and ESR give, when combined with first-principles electronic structure calculations of the second virial coefficient of the ^{129}Xe hyperfine coupling, information on the degrees of electron and nuclear spin polarization [1]. A first-principles multiscale model combining molecular dynamics simulation of the Rb-Xe gas mixture with quantum-chemically preparameterized spin Hamiltonian parameters and propagation of the spin density matrix according to the Liouville-von Neumann equation, can shed light on the roles played by the binary Rb-Xe collisions and the long-lived van der Waals complexes, as well as the magnetic-field strength, on SEOP efficiency. The spin transfer in individual complexes is seen to increase step-wise upon oscillations of the Rb-Xe bond length [2].

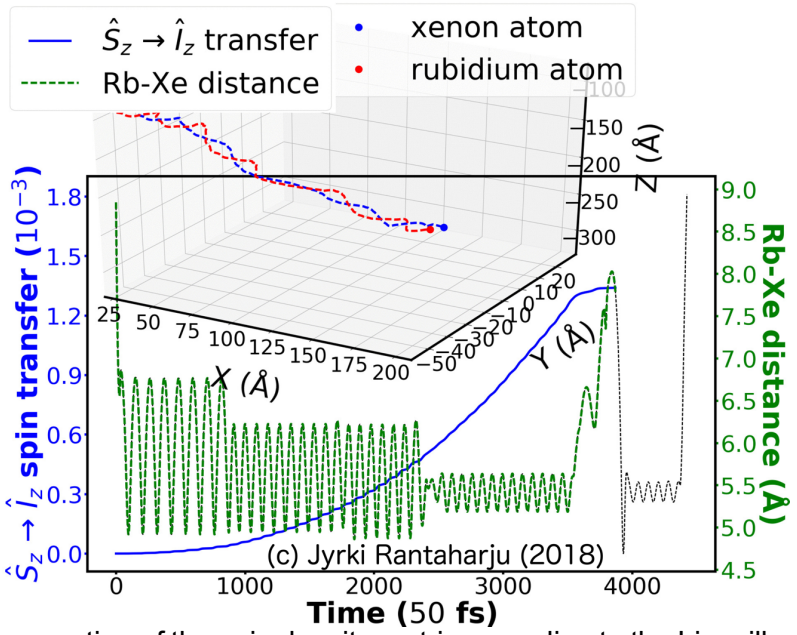

- **temperature dependence of ^{129}Xe chemical shift**: The chemical shift maximum as a function of T of dissolved xenon in aqueous solution is seen to result from a combination of decreasing local solvent density (Xe coordination number) and increasing solute-solvent collision energy, with increasing T [3]. The underlying reason for the latter is the soaring intermolecular chemical shift function in close encounters of Xe and H_2O. Parallel tempering Monte Carlo studies of ^{129}Xe NMR in liquid-crystal (LC) solution confined in cylindrical nanocavities provides detailed information on the orientational and positional order of confined LCs [4].
- **indirect spin-spin coupling in the prototypic van der Waals complex, $^{129}Xe_2$**, can be reliably calculated from first principles provided that both relativity and electron correlation are duly accounted for [5]. Its anisotropy ΔJ can be can be deduced in a solid-state inclusion compound through the experimental effective dipole-dipole coupling, which includes a significant indirect contribution [6].

[1] M. Hanni, P. Lantto, M. Repiský, J. Mareš, B. Saam, and J. Vaara, Phys. Rev. A **95**, 032509 (2017).
[2] J. Rantaharju, M. Hanni, and J. Vaara, *submitted for publication* (2018).
[3] P. Peuravaara, J. Karjalainen, J. Zhu, J. Mareš, P. Lantto, and J. Vaara, *submitted for publication* (2018).
[4] J. Karjalainen, J. Vaara, M. Straka, and P. Lantto, Phys. Chem. Chem. Phys. **17**, 7158 (2015).
[5] J. Vaara, M. Hanni, and J. Jokisaari, J. Chem. Phys. **138**, 104313 (2013).
[6] J. Jokisaari and J. Vaara, Phys. Chem. Chem. Phys. **15**, 11427 (2013).

Third-Generation Automated Clinical-Scale Batch-Mode Xe-129 Hyperpolarizer

Panayiotis Nikolaou[1], Aaron M. Coffey[1], Bryce Kidd[2], Michael Molway,[2] Liana Bales,[2] Megan Murphy[2], Boyd M. Goodson[2], Michael J. Barlow[3], Eduard Y. Chekmenev[1] eduard_chekmenev@hotmail.com

[1]Wayne State University & Karmanos Cancer Center (KCC), Detroit, MI, United States
[2]Southern Illinois University Carbondale, Carbondale, IL, United States
[3]University of Nottingham, Nottingham, United Kingdom

BACKGROPUND: There have been many recent advances in the field of hyperpolarized (HP) noble gas production and imaging, largely enabled by the development of low-cost, high-power frequency-narrowed laser diode arrays (LDAs) and the improvement of ^{129}Xe polarizer technology in general. In particular, our team along with our collaborators previously have developed two generations of clinical-scale hyperpolarizers: an "open-source" prototype, and our "3D-printed" hyperpolarizer--each improving on the previous generation (see References), with the ultimate goal to develop a relatively low-cost, high-capacity Xe hyperpolarizer with fully automated operation that can deliver near-unity Xe nuclear spin polarization—making it attractive for both basic and biomedical research (including for potential clinical use). Here we report on the development and features of the new third-generation batch-mode Xe hyperpolarizer dubbed "XeUS", utilizing Spin Exchange Optical Pumping (SEOP).

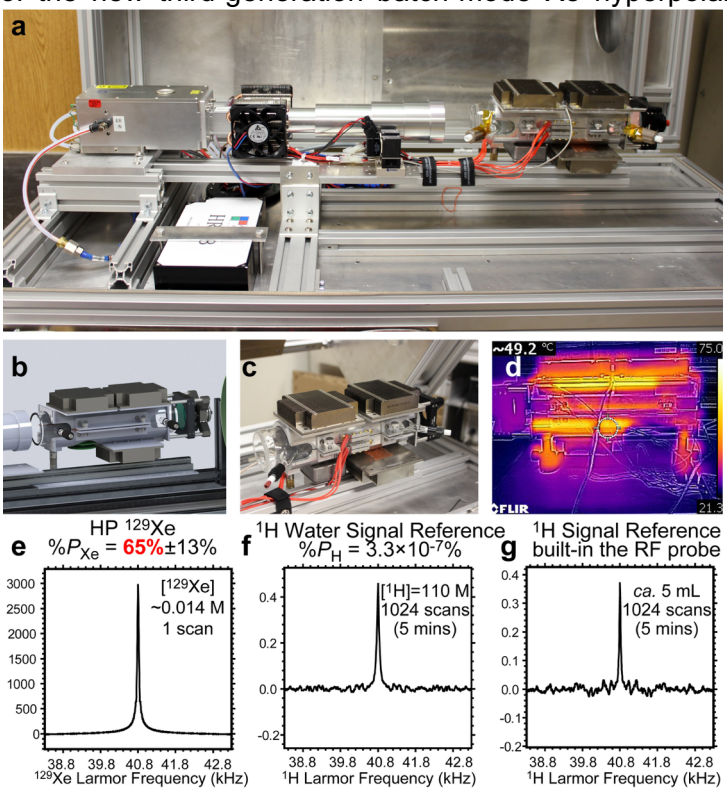

Figure 1. (**a**) Photograph of the actual constructed upper (open) chassis of the Xe hyperpolarizer. (**b**) 3D render pre-production of OP Al heating jacket for heating/cooling. (**c**) Constructed aluminum (Al) jacket with OP-cell, retro-reflection mirror, IR detection, and *in-situ* NMR detection coil and built-in water calibration phantom. (**d**) Infrared thermal image of temperature gradients of Al heating jacket. (**e-g**) *In-situ* NMR spectroscopy at 40.8 kHz: (**e**) ^{129}Xe NMR spectrum of HP ^{129}Xe, (**f**) ^{1}H NMR spectrum thermally polarized water (similar size phantom), and (**g**) ^{1}H NMR spectrum from a thermally polarized built-in phantom comprised of mineral oil.

RESULTS: The new hyperpolarizer operates using a positive-pressure gas manifold with a pre-mixed Xe/N gas cylinder (e.g. using a 50:50 mix), which is employed to load a 0.5 L OP cell to >2000 Torr total gas pressure. This design allows the hyperpolarizer to generate up to 1 L/cycle of HP Xe mixture every ~30 mins. The device chassis is relatively compact: 0.55 m (width) x 1.25 m (length) x 1.35 m (height), and the hyperpolarizer runs on a dedicated single 220 V (20 Amp) circuit, Figure 1. This device utilizes a micro-channel cooled 795 nm, 180 W LDA module (QPC Lasers) with spectral width (FWHM) of <0.2 nm, and with 2" expanding telescope optics to provide homogeneous illumination of the OP cell. The new design employs an aluminum (Al) heating jacket (vs. circulating air) that has direct thermal contact with the OP cell housed within it, which in turn is aligned concentrically to the laser (Figures 1b,c,d). The Al jacket offers several advantages over a conventional forced-air oven: (i) it heats and cools the OP cell significantly faster (<5 mins vs. previous forced-air design of >10 mins), thus reducing polarization cycle times; (ii) it provides rf-shielding for the integrated 40.8 kHz *in-situ* rf coil (see Figure 1e,f,g for in-situ NMR spectroscopy); (iii) it eliminates the need for additional anti-reflection-coated windows typically used in forced-air SEOP ovens (which can cause small but undesirable losses in laser intensity), and (iv) allows for more compact integration of *in-situ* near-IR and NMR sensors. The entire optical path resides in a "light-tight" portion of the chassis. The hyperpolarizer employs a single solenoid NMR magnet that is 8" OD and 22" long.

ACKNOWLEDGMENTS: We thank our collaborator Prof. Matthew S. Rosen (Harvard University). DoD CDMRP Era of Hope Award W81XWH-12-1-0159/BC112431, W81XWH-15-1-0271 and W81XWH-15-1-0272, and 1F32EB021840-01, NSF CHE-1416268 and CHE-1416432, and University of Nottingham (UK) contract.

REFERENCES: (**1**) P. Nikolaou, et al. *JMR* **2009**, *197*, 249. (**2**) N. Whiting, et al. *Appl. Phys. B-Lasers Opt.* **2012** *106*, 775. (**3**) P. Nikolaou, et al. *PNAS* **2013**, *110*, 14150. (**4**) P. Nikolaou, et al. An*al. Chem*. **2014**, *86*, 8206. (**5**) P. Nikolaou, et al. *JPCB* **2014**, *118*, 4809. (**6**) P. Nikolaou, et al. *JACS* **2014**, *136*, 1636. (**7**) P. Nikolaou, et al. *Magn. Reson. Imaging* **2014**, *32*, 541. (**8**) P. Nikolaou, et al. *Chem. Eur. J*. **2015**, *21*, 3156. (**9**) D. A. Barskiy, et al. *Chem. Eur. J*. **2017**, *23*, 725.

Title: Separation of noble gases using Metal Organic Frameworks

Authors: Praveen K. Thallapally, Debasis Banerjee and Michael Sinnwell, Pacific Northwest National Laboratory, Richland, WA, 99352, praveen.thallapally@pnnl.gov

Abstract:

Separation of volatile radionuclides from the off-gas streams of a used nuclear fuel reprocessing facility has been a topic of significant research. The current technology uses energy intensive cryogenic distillation, which is expensive. Another downside of this approach is the accumulation of ozone due to radiolysis of oxygen. Therefore, alternate technologies, and associated materials, are needed for separation of noble gases selectively over other gases including CO_2, N_2, O_2 and Ar (**Figure 1**). Pacific Northwest National Laboratory is exploring a new class of materials called metal organic frameworks for separation of noble gases selectively at near room temperature. Our laboratory results demonstrate the removal Xenon with high adsorption capacity and selectivity compared to benchmark materials, such as zeolites and activated carbons. The high selectivity towards Xe over other gases at low concentration indicates the perfect match between the pore size and the kinetic diameter of the gas species. In this talk I will focus on recent results from our laboratory on separation of noble gases from process off gases at near room temperature using porous metal organic frameworks (**Figure 1**).

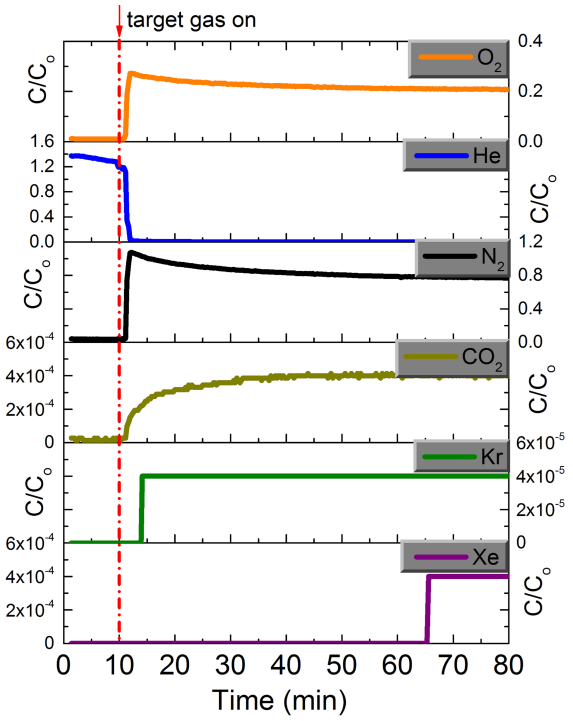

Figure 1. Selective removal of Xenon at room temperature from gas mixture using metal organic framework.

References:

1) Banerjee D, CM Simon, SK Elsaidi, M Haranczyk, and **PK Thallapally**. 2018. "Xenon Storage and Separation using Metal Organic Frameworks." *CHEM.,* doi.org/10.1016/j.chempr.2017.12.025. 2) Elsaidi SK, MH Mohamed, CM Simon, E Braun, T Pham, KA Forrest, W Xu, D Banerjee, B Space, MJ Zaworotko, and **PK Thallapally**. 2017. "Effect of Ring Rotation upon Gas Adsorption in SIFSIX." *Chemical Science,* 8, 2373. 3) Feng X, Z Zong, S Elsaidi, JB Jasinski, R Krishna, **PK Thallapally,** and MA Carreon. 2017. "Kr/Xe Separation over a Chabazite Zeolite Membrane." *J. Am. Chem. Soc.,* **138, 9791-9794.** 4) Banerjee D, CM Simon, AM Plonka, RK Motkuri, J Liu, X Chen, B Smit, JB Parise, M Haranczyk, and **PK Thallapally**. 2016. "Metal-organic framework with optimally selective xenon adsorption and separation." *Nature Communications,* 7, DOI:10.1038/ncomms11831. 5) Reiss P, L Chen, D Holden, K Jelfs, S Chong, T Hasell, M Thomas, J Armstrong, J Bell, J Busto, R Noel, J Liu, DM Strachan, **PK Thallapally,** and A Cooper. 2016. "Rare gas separation by a dynamic molecular filter." *Nature Materials,* 13, 954-960. 6) Banerjee D, AJ Cairns, J Liu, RK Motkuri, SK Nune, CA Fernandez, R Krishna, DM Strachan, and **Thallapally, PK**. 2015. "Potential of Metal-Organic Frameworks for Separation of Xenon and Krypton." *Acc. Chem. Res.,* 48, 211-219.

In Situ ^{129}Xe NMR Spectroscopy of Flexible MOFs

E. Brunner,*[1] S. Kaskel,[2] F. Kolbe,[1] S. Krause,[2] S. Paasch,[1] M. Rauche,[1] I. Senkovska[2]

[1] TU Dresden, Faculty of Chemistry and Food Chemistry, Bioanalytical Chemistry, 01062 Dresden, Germany
[2] TU Dresden, Faculty of Chemistry and Food Chemistry, Inorganic Chemistry I, 01062 Dresden, Germany

* Presenting Author, E-mail: eike.brunner@tu-dresden.de

Background: Metal-Organic Frameworks (MOFs) exhibit unique properties, for example huge internal surfaces. A particularly important sub-class of MOFs is surprisingly flexible. Such compounds undergo pronounced, adsorption-induced structure transitions and can change their unit cell volumes by more than a factor of two. This process depends on the temperature, gas pressure, and type of adsorbed gas and is not yet fully understood.

Methods: Within the present contribution, we describe ^{129}Xe NMR studies of flexible MOFs. *In situ* studies of host-guest interactions are particularly powerful. Our homebuilt apparatus [1] allows *in situ* high-pressure NMR spectroscopic studies by the application of variable gas pressures up to a relative pressure of 1 at variable temperatures down to 190 K inside the NMR spectrometer. This allows following adsorption/desorption isotherms by observing the signals of the adsorbed gases and to correlate the NMR-derived parameters with volumetric measurements.

Results: The described *in situ* NMR technique could for example be used to characterize xenon-induced phase-transitions in the recently discovered pressure-amplifying framework material DUT-49 with its unique negative gas adsorption transitions [2,3]. Xenon is capable of inducing mesopore closure at increasing pressure and 200 K resulting in gas release, i.e., negative gas adsorption. Gas exchange processes are studied by 2D exchange spectroscopy (EXSY).

Furthermore, we have used a combination of *in situ* high-pressure NMR spectroscopy and ^{13}C CP MAS NMR spectroscopy in order to elucidate the structural reasons for the fact, that the compound DUT-8(Ni) can be synthesized either as a flexible MOF with a huge change of the unit cell volume during gating transition or as a fully rigid material [4]. It is also demonstrated that the chemical shift of ^{129}Xe observed at very high pressure, i.e., close to a relative pressure of 1, correlates well with the average pore size of MOFs [5] and can thus be used as a measure to estimate average pore sizes.

Conclusions: In summary, the combination of *in situ* high-pressure NMR spectroscopy, solid-state NMR spectroscopy, and volumetric xenon adsorption experiments provides deeper insight into the unique adsorption and phase transition behavior of flexible MOFs like DUT-49 and DUT-8.

Funding Sources: Financial support from the Deutsche Forschungsgemeinschaft (Research Unit FOR 2433 "*MOFswitches*") is gratefully acknowledged.

References:

[1] H. Hoffmann, B. Assfour, F. Epperlein, N. Klein, S. Paasch, I. Senkovska, S. Kaskel, G. Seifert, E. Brunner, *J. Am. Chem. Soc.* **133** (2011) 8681.
[2] S. Krause, V. Bon, I. Senkovska, U. Stoeck, D. Wallacher, D. Többens, S. Zander, R. Pillai, G. Maurin, F.-X. Coudert, S. Kaskel, *Nature* **532** (2016) 348.
[3] J. Schaber, S. Krause, S. Paasch, I. Senkovska, V. Bon, D. Toebbens, D. Wallacher, S. Kaskel, E. Brunner, *J. Phys. Chem. C* **121** (2017) 5195.
[4] N. Kavoosi, V. Bon, I. Senkovska, S. Krause, C. Atzori, F. Bonino, J. Pallmann, S. Paasch, E. Brunner, S. Kaskel, *Dalton Trans.* **49** (2017) 4685.
[5] K. Trepte, J. Schaber, S. Schwalbe, F. Drache, I. Senkovska, S. Kaskel, J. Kortus, E. Brunner, G. Seifert, *Phys. Chem. Chem. Phys.* **19** (2017) 10020.

Using ^{129}Xe NMR and hyperCEST for Biological Sensing

David Wemmer, Alex Pines, Matthew Francis, Clancy Slack, Joel Finbloom, Keunhong Jeong, Muller Gomes
Department of Chemistry, University of California, Berkeley CA 94720

The very now natural occurrence of xenon, and the ability to hyperpolarize the nuclei of ^{129}Xe make this rare gas very attractive for experiments with NMR detection. Its inertness also makes it excellent as a biological probe. Many applications with hp-^{129}Xe have shown that its chemical shift is highly sensitive to environment, allowing it to report on binding sites accessible to it. To adapt this approach to detection of specific biological targets we developed the concept of a xenon biosensor, an adaptor molecule that interacts with a target of interest with high specificity but also carries a xenon-binding element. Initial experiments used modified cryptophane-A as the binding element for several different kinds of targeting agent. Exchange of xenon in and out of cryptophane is at a convenient rate to allow saturation transfer to be done, that can be used to enhance contrast for imaging. Using multiple Xe binding elements per targeting element allows detection into the pM concentration range. We will show applications of this approach in biological sensing of specific cells and targets.

Other xenon binding compounds are known, and over the past few years cucurbits have been demonstrated as CEST agents. These compounds offer possible ways to introduce specificity through chemical reactivity. We will discuss detection based on cleavage of a blocking group that can be used to report on the presence of a protease, for example. Many other reactions can be envisioned.

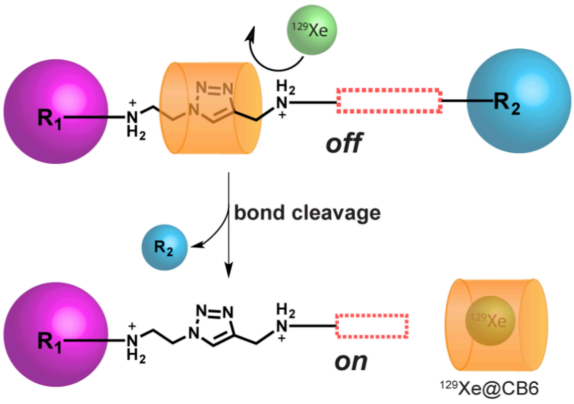

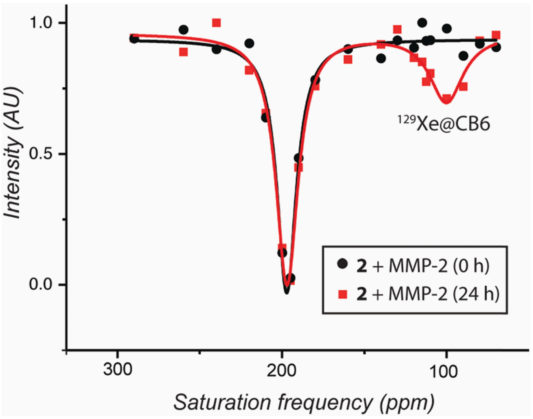

We have also explored detecting interactions using xenon relaxometry. While this does not provide such high specificity, relaxation measurements can be extended to very low fields with non-NMR detection that could offer advantages in some contexts. An example of this for detection of drug-protein interaction will be given.

Slack, CC et al., Chem Commun. 2017, 53, 1076.

Contrast Agents with “ideal“ dynamic range scaling behavior for hyperpolarized xenon MRI

Martin Kunth[†], George J. Lu[†], Christopher Witte[‡], Leif Schröder[‡], Mikhail G. Shapiro[†]

[†]California Institute of Technology, Division of Chemistry and Chemical Engineering, Pasadena, California 91125, USA; [‡]Leibniz-Forschungsinstitut für Molekulare Pharmarkologie (FMP), 13125 Berlin, Germany

Email address of presenter: mkunth@caltech.edu

Background: Magnetic resonance imaging (MRI) contrast agents acting on hyperpolarized nuclei such as xenon-129 (^{129}Xe) can be detected at orders of magnitude lower concentrations than conventional MRI reporters. However, the variable concentration of hyperpolarized nuclei delivered to biological specimens presents a fundamental challenge for the use of hyperpolarized MRI contrast agents in quantitative molecular imaging. Here we show that a recently discovered class of genetically encoded reporters for hyperpolarized ^{129}Xe-MRI overcomes this limitation through an elastic binding capacity for xenon. These reporters are based on gas vesicles (GVs) — microbe-derived, gas-filled protein nanostructures [1]. We show that the xenon binding capacity of gas vesicles follows the ideal gas law, allowing their contrast under hyperpolarized xenon chemical exchange saturation transfer (Hyper-CEST) imaging [2] to scale linearly with total xenon signal (Fig. (a)). This response allows the production of MRI contrast that is robust to variability in the concentration of xenon, and enables virtually unlimited improvement in absolute contrast with increased xenon delivery. These properties provide an “ideal” dynamic range scaling for use in emerging biochemical and *in vivo* imaging applications of hyperpolarized xenon MRI.

Methods: Quantitative xenon Hyper-CEST MRI [3] for varying free xenon concentration was performed on three types of gas vesicle nanostructures which were derived either from bacteria *Anabaena flos-aquae* (*Ana*), *Halobacterium salinarum* (*Halo*) and *Bacillus megaterium* (*Mega*), and dissolved in phosphate buffered saline solution (PBS). A sample of 10 µM of Cryptophane-A (CrA) in PBS served as control. *z*-Spectra were analyzed for the on-average number of xenon atoms that were bound to each particular xenon-host similar to [4].

Results: For the CrA control, the relative magnitude of the CEST effect decreased with increasing total xenon gas pressure. In contrast, *z*-spectra from GVs were invariantly constant, revealing a linear increase in hosted xenon atoms per GV (Fig. (b)).

Conclusions: This observed behavior can be explained by a thermodynamic equilibrium between xenon in the solution and in GVs determined by the Ostwald solubility coefficient of the gas. This enables a virtually unlimited scaling of the magnetization in the CEST pool and yields a self-compensating elasticity of the saturation transfer, *i.e.*, stable contrast with variable xenon delivery. The linear scaling we observed for the partitioning between free bulk xenon and GV-bound xenon applies in general to all systems that rely on partitioning into different spaces that provide a different chemical shift, rather than bimolecular binding (including perfluorooctyl bromide nanodroplets [5] and bacterial spores [6]).

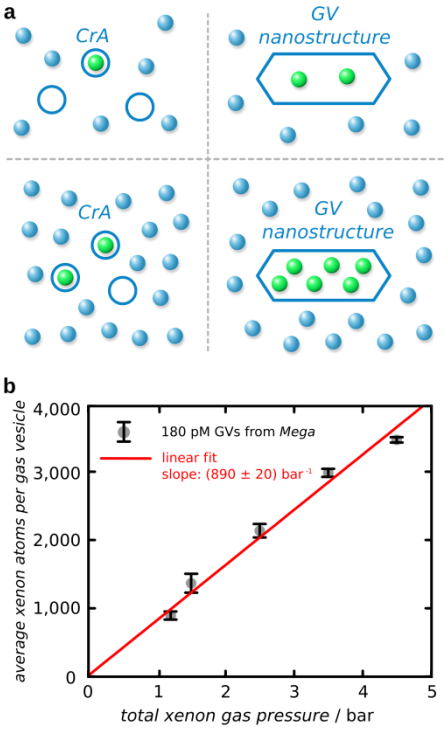

Source(s) of Funding: Human Science Frontier Program (HSFP) no. RGP0050 to LS and MGS.

References: [1] Shapiro *et al.* **Nat. Chem.** 6, 629 (2014); [2] Schröder *et al.* **Science** 314, 446 (2006); [3] Kunth *et al.* **JCP** 141, 194202 (2014); [4] Kunth *et al.* **Chem. Sci.** 6, 6069 (2015); [5] Stevens *et al.* **JACS** 135, 9576 (2013); [6] Bai *et al.* **Chem. Sci.** 5, 3197 (2014).

Small molecule-based biosensors for ^{129}Xe NMR

Serge D. Zemerov, Yanfei Wang, Brittany A. Riggle, Benjamin W. Roose, Mara L. Greenberg, Rebecca F. Wissner, John P. Philbin, Jordan L. Doman, E. James Petersson, and Ivan J. Dmochowski

Department of Chemistry, University of Pennsylvania, 231 S 34th St., Philadelphia, PA 19104
zemerov@sas.upenn.edu

Background: Magnetic resonance imaging (MRI) is a widely used tool for the detection and diagnosis of various disease states, but is limited in its use in imaging low-abundance biomarkers. Over the past two decades, hyperpolarized (hp) ^{129}Xe NMR and MRI have been investigated as complements to traditional ^{1}H-based techniques in attempts to increase detection sensitivity. Hp ^{129}Xe, readily achieved by the process of spin-exchange optical pumping, can reach 10^5 signal enhancement over the thermally polarized Boltzmann population of nuclear spins.[1] Our lab and others have exploited xenon's great sensitivity to its molecular environment *via* the design of xenon hosts that generate a unique ^{129}Xe NMR chemical shift upon association with their target. Here, we present three different small molecule-based biosensors that have been shown to label cells in acidic microenvironments (Fig. 1a),[2] detect specific proteins *via* a molecular relay (Fig. 1b),[3] and function as a "turn-on" biosensor for the protein calmodulin (Fig. 1c).[4]

Methods: Hyperpolarized (hp) ^{129}Xe was generated using the spin-exchange optical pumping method with a home-built ^{129}Xe polarizer. A Shark 65 W tunable ultra-narrow band diode laser set to 795 nm was used for optical pumping of Rb vapor. A gas mixture of 89% helium, 10% nitrogen, and 1% natural abundance xenon was used as the hyperpolarizer input. ^{129}Xe hyperpolarization level was roughly 10-15%.

Results: At pH 5.5, the EALA-repeat peptide appended to WEC (Fig. 1a) became α-helical and was able to insert into the membranes of HeLa cells. This insertion resulted in a 13.4 ppm downfield chemical shift relative to a solution of biosensor and cells at pH 7.5. This illustrates the ability of this construct to target extracellular acidic pH as a cancer biomarker. Additionally, we designed two-faced guest (TFG) molecules that initially bind inside the cavity of cucurbit[6]uril (CB[6]), blocking the Xe@CB[6] signal. Due to the higher affinity of the TFG for the protein analyte carbonic anhydrase II (CAII) than CB[6], we showed that in the presence of CAII the TFG was bound by the protein, allowing Xe access to the cavity and producing the Xe@CB[6] signal. This molecular relay has potential to be reprogrammed for assaying a wider range of protein targets. Finally, we showed that the functionalized cryptophane FRRIAR-TUC is a "turn-on" biosensor capable of detecting Ca^{2+}-bound calmodulin (CaM). FRRIAR-TUC alone and in the presence of apo CaM resulted in no ^{129}Xe NMR signal, while holo CaM bound to FRRIAR-TUC resulted in two distinct peaks (Fig. 1c).

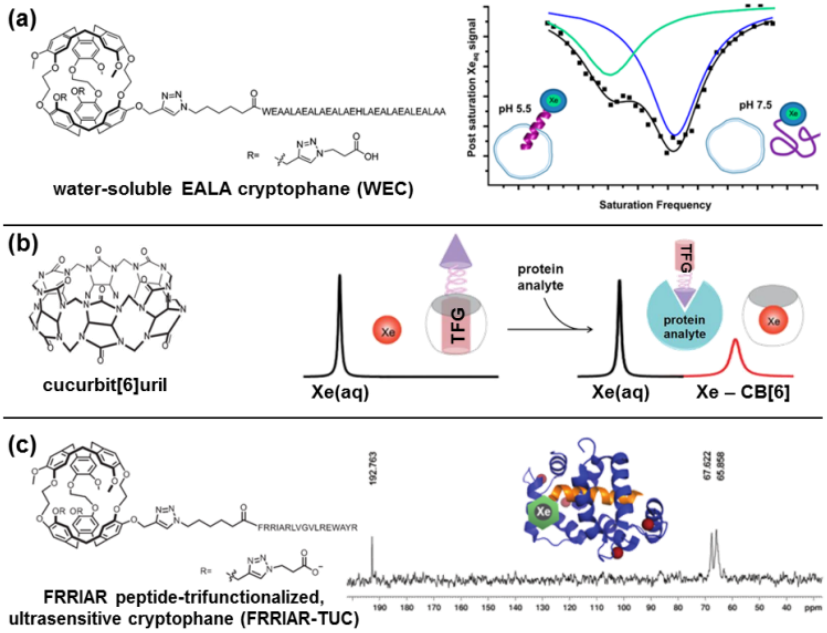

Figure 1. The small molecule-based biosensors WEC (a), cucurbit[6]uril + two-faced guest (TFG) molecular relay (b), and FRRIAR-TUC (c).

Conclusions: The use of small molecules in ^{129}Xe biosensing applications is an exciting technique with strong potential for ultrasensitive (nM-pM) detection of biomedically relevant analytes, as well as high specificity for the target of interest. Further investigation into the molecular mechanism behind ^{129}Xe chemical shift changes should allow for the design of biosensors with predetermined Xe@host chemical shifts, allowing for multiplexed detection.

Funding: NIH R01-GM097478; CDMRP-LCRP Concept Award No. LC130824; GM097478S1

References: [1] Walker, T. G.; Happer, W. *Rev. Mod. Phys.* **1997**, *69* (2), 629. [2] Riggle, B. A. et al. *J. Am. Chem. Soc.* **2015**, *137* (16), 5542. [3] Wang, Y. et al. *Angew. Chemie - Int. Ed.* **2016**, *55* (5), 1733. [4] Riggle, B. A. et al. *Org. Biomol. Chem.* **2017**, *15*, 8883.

Experimental determination of pore shapes using phase retrieval from the q-space imaging signal of diffusing ^{129}Xe gas

Kerstin Demberg[1]*, Frederik B. Laun[2], Peter Bachert[1] and Tristan A. Kuder[1]

[1] Medical Physics in Radiology, German Cancer Research Center, Heidelberg, Germany
[2] Institute of Radiology, University Hospital Erlangen, Friedrich-Alexander-Universität Erlangen-Nürnberg, Erlangen, Germany
* k.demberg@dkfz-heidelberg.de

Background: The average shape of arbitrary closed pores filled with an NMR-detectable medium contained in an imaging volume element can be measured with NMR diffusion pore imaging [1]. Probing porous microstructures, e.g. reservoir rocks or tissue cells, with classical single diffusion encoding composed of two short gradient pulses, known as q-space imaging, only yields the squared magnitude of the Fourier transform of the pore image [2] entailing an inversion problem: An unambiguous reconstruction of the pore image requires both magnitude and phase. Until now, experimentally challenging phase measurements using specialized temporal gradient profiles were a prerequisite to obtain the full information in Fourier space. In this work, the phase information is recovered from the magnitude by applying a phase retrieval algorithm that is commonly used in the analysis of X-ray scattering measurements.

Methods: The phase was retrieved iteratively using the hybrid input-output algorithm [3] plus shrinkwrap extension [4]: Starting with a random image, repeated Fourier transforms between image and q space were performed while imposing corrections to the new estimates in each domain: In q space, consistency with the magnitude was imposed, while in image space, the pore was constrained to a finite extent, which is an essential assumption to enable phase retrieval. Hyperpolarized ^{129}Xe gas was used in controlled phantom experiments for validation.

Results: The phase retrieval approach proved to be successful in solving the phase problem in diffusion pore imaging and proved to be very stable in the presence of noise. The figure shows an example of a phantom with star-shaped pores: The respective q-space magnitude was fed to the algorithm to retrieve the desired Fourier phase which allows computation of the pore image.

Conclusions: The phase retrieval approach, solely employing q-space imaging, reduces acquisition time and might eliminate the experimentally challenging phase measurements: Applying q-space gradients is particularly easy and flexible, technically stable and could be advantageous for imaging tissue microstructure *in vivo*, where cardiac driven pulsation and patient movement complicate phase measurements.

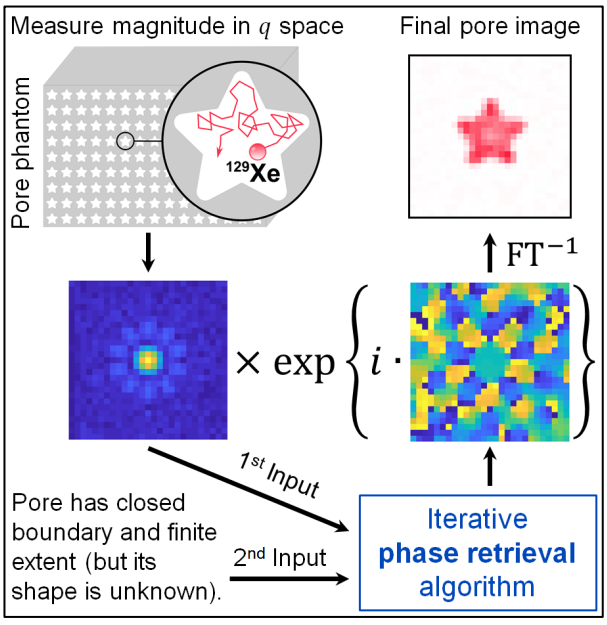

Funding: Financial support by the DFG (grant no. KU 3362/1-1 and LA 2804/6-1) is gratefully acknowledged.

References:

[1] F.B. Laun, T.A. Kuder et al., Phys. Rev. Lett. 107, 048102 (2011).
[2] P.T. Callaghan, A. Coy et al., Nature 351, 467 (1991).
[3] J.R. Fienup, Opt. Lett. 3, 27 (1978).
[4] S. Marchesini, H. He et al., Phys. Rev. B 68, 140101(R) (2003).

Assessing hidden structures of metal organic polyhedra (MOP) using ^{129}Xe Hyper-CEST

Jabadurai Jayapaul[1], Sanna Komulainen[2], Vladimir Zhivonitko[2], Perttu Lantto[2], Kari Rissanen[3], Ville-Veikko Telkki[2], and Leif Schröder[1]

[1] *Molecular Imaging, Leibniz-Forschungsinstitut für Molekulare Pharmakologie (FMP), 13125 Berlin, Germany*
[2] *NMR Research Unit, University of Oulu, 90014 Oulu, Finland*
[3] *University of Jyväskylä, Department of Chemistry, 40014 Jyväskylä, Finland. Email:jayapaul@fmp-berlin.de*

Self-assembly of different sub-components with metal cations in solution produces discrete metal complexes called metal-organic polyhedra (MOP). These components enable formation of hydrophobic cavities in MOPs. MOP cavities play an important role in molecular recognition[1], gas adsorption and separation[2] and in binding hydrophobic guests via inclusion complexation. Even though a Fe-MOP was reported to reversibly encapsulate hydrophobic Xe gas[2], the three theoretically possible conformers of Fe-MOP remained partially undetected under these conditions. Therefore, we utilized highly sensitive hyperpolarized (HP) ^{129}Xe in combination with chemical exchange saturation transfer (CEST) i.e. Hyper-CEST technique[3] for detection of even trace Fe-MOP conformers in "hidden states".

Since Fe-MOP is a self-assembled host, inspecting its supramolecular stability under different perturbation conditions (e.g., temperature, blocking (Guanidinium chloride, Gu.HCl), competition (cyclohexane (Cyhex), SF_6) using HP ^{129}Xe guest will be of special interest. Subsequently, the Fe-MOP was extensively investigated for identifying its hidden conformers using direct Xe-NMR and by Hyper-CEST, respectively. Theoretical calculations were performed to explain the observed complex CEST spectra.

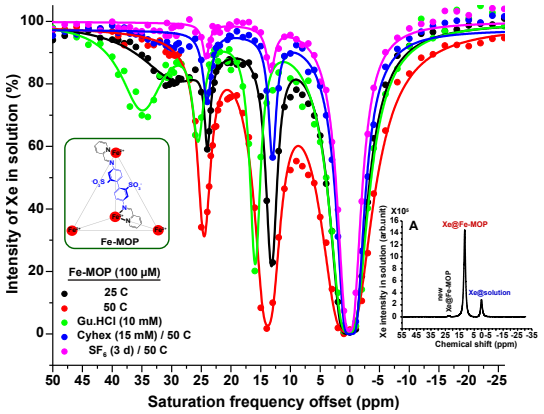

Figure 1. The Fe-MOP structure with one coordinating ligand (for clarity) is shown in the inset. Z spectra of Fe-MOP (100 μM) at 25 and 50 °C, and under blocking (Gu.HCl (10 mM)) or competition (Cyhex (15 mM) or SF_6) conditions. Direct HP Xe-NMR of Fe-MOP (10.3 mM) revealed a new and less intense Xe-bound peak at 24 ppm (A).

The water-soluble tetrahedral Fe-MOP was synthesized according to literature[4]. Hyper-CEST (z-spectra) of Fe-MOP (100 μM) at 25 °C showed three CEST peaks at 13, 24 and 30 ppm, respectively (Fig. 1). Cycling the temperature of Fe-MOP (100 μM) from 25 to 50 °C and cooling back to 25 °C inferred different Xe exchange rates and regenerated the starting CEST conditions (Fig. 1). Various control experiments confirmed that the origin of 3 CEST peaks might arise due to Fe-MOPs hidden conformers. Blocking exterior of Fe-MOP (100 μM) using Gu.HCl (10 mM) revealed left shift of 3 CEST peaks and altered Xe exchange rate (Fig. 1). Providing competing, larger, strong binding guests (Cyhex (15 mM), SF_6 (3 days)) to Fe-MOP (100 μM) along with Xe at 50 °C exhibited reduction in peak intensities (∼30 - 60 %) at 13 and 24 ppm (Fig. 1). Direct Xe-NMR of Fe-MOP (10.3 mM) indicated a less intense new Xe-bound peak at 24 ppm (Fig. 1A). Selective inversion recovery experiments illustrated that both cage signals are mainly connected through exchange via the solution pool but not through direct conversion. Quantum chemical and DFT calculations suggest that the reproducible and consistent 3 CEST peaks could arise due to Fe-MOPs three conformers.

In summary, Fe-MOP remained intact while being perturbed by temperature cycling and Xe entered the Fe-MOP cavity in spite of blocking and competing larger guests. We could show for the first time a new Xe-bound peak (24 ppm) by direct Xe-NMR and consistent, reproducible 3 CEST peaks by Hyper-CEST that might originate from 3 conformers of Fe-MOP.

References

[1] A.C. Sudik et.al, JACS, **2005**, 127, 7110-7118.
[2] J. Roukala et.al, JACS, **2015**, 137, 2464-2467.
[3] P.Mal, *Angew. Chem. Int. Ed.*, **2015**, 54, 2806-2810.
[4] C. Witte et.al, *Angew. Chem. Int. Ed.*, **2008**, 47, 8297-8301.

^{129}Xe probing metallosupramolecular and porous organic cages as well as hydrated cements and natural shales

Sanna Komulainen,[a] Juho Roukala,[a] Jianfeng Zhu,[a] Vladimir V. Zhivonitko,[a] Muhammad Asadullah Javed,[a] Bing Zhou,[b] Linjiang Chen,[c] Daniel Holden,[c] Tom Hasell,[c] Andrew Cooper,[c] Chandan Giri,[d] Kari Rissanen,[d] Juha Vaara,[a] Perttu Lantto,[a] Ville-Veikko Telkki[a]

[a]*NMR Research Unit, University of Oulu, Finland*
[b]*School of Materials Science and Engineering, Tongji University, Shanghai, China*
[c]*Department of Chemistry, Centre for Materials Discovery, University of Liverpool, UK*
[d]*Department of Chemistry, Nanoscience Center, University of Jyväkylä, Finland*

e-mail: ville-veikko.telkki@oulu.fi

Xenon is an excellent probe for characterizing structures of porous materials because of its inertness and the high sensitivity of ^{129}Xe chemical shift to its local environment. Recently, we have exploited various experimental ^{129}Xe NMR techniques accompanied by state-of-the-art quantum chemical modelling to investigate properties of topical materials. This talk highlights our observations.

Water-soluble tetrahedral Fe_4L_6 cage[1] has been used as a container molecule for air-sensitive molecules, like white phosphorus.[2] Our ^{129}Xe NMR experiments show that the Fe_4L_6 cage can encapsulate xenon.[3] The observation pave the way for exploiting metallosupramolecular cages as economical means to extract rare gases as well as ^{129}Xe NMR based bio-, pH and temperature sensors.

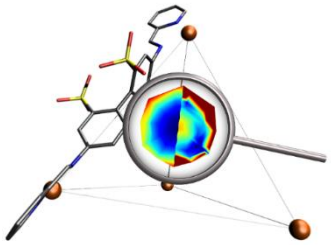

A solid porous molecular crystal formed from an organic cage, CC3, has unprecedented performance for the separation of rare gases.[4] We used xenon as an internal reporter providing extraordinarily versatile information about the gas adsorption phenomena in the cage and window cavities of the material.[5]

We have exploited, for the first time, ^{129}Xe NMR to investigate the nanoscale porous structures in hydrated white cements and natural shale.[6] The shale spectra include a very broad signal, covering a range of about 600 ppm, implying that the adsorbed xenon interacts with the paramagnetic centers present in the samples.

Funding
Academy of Finland, grant numbers 289649 and 294027, and H2020 European Research Council (ERC), grant number 772110.

References

[1] P. Mal, D. Schultz, K. Beyeh, K. Rissanen, J. R. Nitschke, *Angew. Chem. Int. Ed*. 2008, **47**, 8297.
[2] P. Mal, B. Breiner, K. Rissanen, J. R. Nitschke, *Science* 2009, **324**, 1697.
[3] J. Roukala, J. Zhu, C. Giri, K. Rissanen, P. Lantto, V.-V. Telkki, *J. Am. Chem. Soc*. 2015, **137**, 2464.
[4] T. Tozawa *et al*, *Nat. Mater*. 2009, **8**, 973.
[5] S. Komulainen, J. Roukala, V. V. Zhivonitko, M. A. Javed, L. Chen, D. Holden, T. Hasell, A. Cooper, P. Lantto, V.-V. Telkki, *Chem. Sci.* 2017, **8**, 5721.
[6] B. Zhou, S. Komulainen, J. Vaara, V.-V. Telkki, *Micropor. Mesopor. Mat*. 2017, **253**, 49.

Xe atom: The spy that came in from the cold

Cynthia J. Jameson

University of Illinois at Chicago cjjames@uic.edu

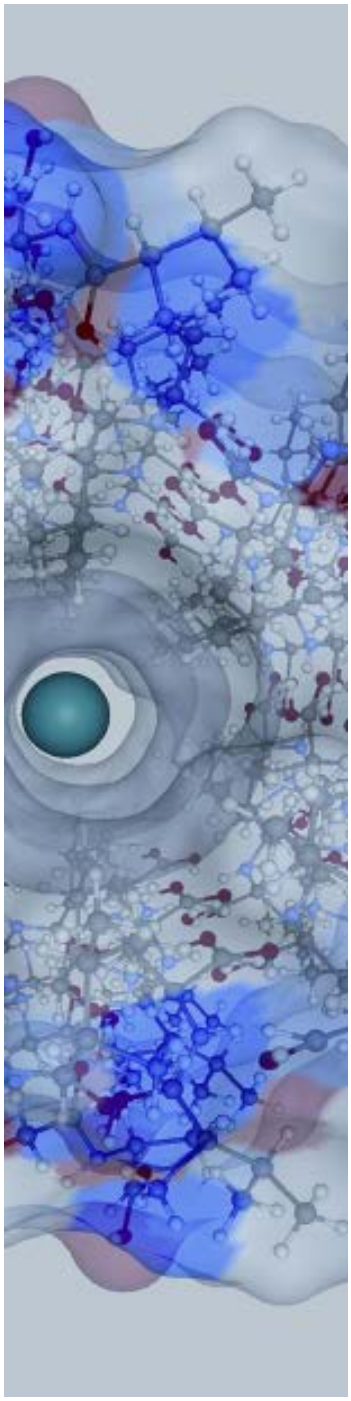

Background: Xe intermolecular chemical shifts are exquisitely sensitive to the environment of the Xe atom. This permits the Xe nucleus to encode and report attributes of the physical system in which Xe atom finds itself. In order to elicit the desired detailed information about the physical system, the observed Xe chemical shifts relative to the free Xe atom need to be understood at a fundamental level.

Approach: At first we send out our spy into clear-cut scenarios (model physical systems with well-established structures) where other sources (experiments and calculations) can provide checks and double checks on the information, and in this process set up the encryption codes (quantitative fundamental understanding of the Xe chemical shift for such model systems), then debriefing (physical insights connecting calculations to experiments in the model systems) reveals the quality/reliability of the detailed information in those clear-cut scenarios. Thereafter, we can send our spy into uncharted territory where no double checks may be possible, yet we have our previous calibrations on the reliability of the transcription which lets us derive some useful information (situation report) from the field.

Methods: Theoretical calculations use quantum mechanical methods that include electron correlation, some relativistic corrections as needed, using a very large basis set for the Xe atom, including high orbital angular momentum functions that are required for Xe electron distribution to properly respond to any neighboring atoms, properly describe the environment by including long-range effects such as hydrogen-bonding networks, include position dependence in the quantum calculations to permit dynamic averaging, and where appropriate carry out molecular dynamics or Monte Carlo simulations for proper dynamic averaging as a function of temperature.

Results: We will present some model systems examples that provide physical insight into what the chemical shift is telling us about the environment, so that some generalization may be possible. We will ask physical aspects questions and find answers from calculations that reproduce experiments.

Conclusions: Encoded in the intrinsic Xe shielding response surface is the electronic structure of the system (a supermolecule or a crystal fragment) as a function of nuclear configuration. The dynamic averaging encodes further information about the nuclear environment into the observed chemical shift. It is possible to use a combination of quantum mechanical calculations and grand canonical Monte Carlo or MD simulations in model systems in order to understand the Xe chemical shifts. From such understanding may come some insight into the encoded information in more complex, real-world systems. The information that is encoded in observed Xe spectra are structural as well as dynamic information. Where Xe travels in nanochannels, it provides information on the diameter of the channel, the aspect ratio of the cross section of the channel, the architecture of the channel. Where Xe resides in a cage, it provides information on the average size of the cage, the average symmetry of the cage, the number of other molecules per cage with it, the electronic structure of atoms constituting the cavity walls, the environment outside a deformable cage.

References: C. J. Jameson website: http://www.stemwomen.org/pubs.html

A comprehensive Hyper-CEST model: experiment control and quantitative data evaluation

Sergey Korchak,[a] T. Riemer,[b] Wolfgang Kilian[a] and Lorenz Mitschang[a]
[a]Physikalisch-Technische Bundesanstalt (PTB), 10587 Berlin, [b]University of Leipzig, 04107 Leipzig

Hyperpolarized ^{129}Xe in conjunction with molecular host structures where it can reversibly bind to is a formidable magnetic resonance probe for the targeting of biomolecular and cellular markers. This biosensing approach is already qualitatively established in a number of in vitro investigations.[1] Here, an analytical model of the underlying measurement process is presented to enable progress towards tailored and quantitative applications.

Biosensors are detected through the signal of freely dissolved xenon based on the saturation transfer from sensor-bound xenon.[2] In the model $S(\rho,\tau,\omega)$ for this process, the free xenon concentration within the solution, ρ, the duration of RF saturation, τ, and the xenon nutation frequency in the saturating RF, ω, are variables quite freely adjustable by the experimenter:

$$S(\rho,\tau,\omega) = A_0(\rho)\ e^{-R\tau} - A_0(\rho)\ e^{-[R+r_{on}(\rho,\omega)]\tau}$$

The first term is the signal due to free xenon when no saturation transfer applies, with R for the xenon relaxation rate, and $A_0(\rho)$ for the initial magnetization density which reflects the xenon hyperpolarization; in the second term saturation transfer is included through the rate r_{on} which is the product of the xenon transition rate from the free to sensor-bound state and a scaling factor accounting for the saturation efficiency. Overall, the saturation transfer rate r_{on} is governed by kinetic parameters related to the underlying exchange mechanism, the rate coefficients for dissociative and degenerate exchange processes and the xenon binding affinity to the sensor,[3] as well as ρ and ω and the concentration of total sensor in the solution. For a given sensor, the kinetic parameters, R, and $A_0(\rho)$ may be determined by dedicated experimentation to evaluate together with the settings for ρ, τ, ω, and the given sensor concentration, Hyper-CEST (Fig. 1).

As demonstrated for the xenon host-molecule cryptophan-A in aqueous solution,[4] the approach could be useful in a wide range of sensing applications, e.g. to forecast experimental results or to optimize the experiment performance. Furthermore, by inversion of the model, evaluation of parameters from experimental data becomes possible, e.g. the total sensor concentration – and thus possibly the amount of the targeted molecule in the solution – can be absolutely quantitated. Functional extension of S for in vivo applications by encompassing the physiology of xenon distribution and sensor localization in the organism appears feasible, whereas strategies for the specification of the required model parameters are lacking.

Acknowledgements This work was funded by EURAMET (01EZ1010A) and the German Science Foundation (TRR 676-A2).

References

1. L. Schroeder, T. J. Lowery, C. Hilty, D. E. Wemmer & A. Pines, Science 314, 446 (2006). Y. Wang & I. J. Dmochowski, Acc Chem Res 49, 2179 (2016).
2. M. Zaiss, M. Schnurr, P. Bachert, *J Chem Phys* 136, 144106 (2012).
3. S. Korchak, W. Kilian, L. Schröder & L. Mitschang, J Magn Reson 265, 139 (2016).
4. S. Korchak, T. Riemer, W. Kilian & L. Mitschang, Phys Chem Chem Phys 20, 1800 (2018).

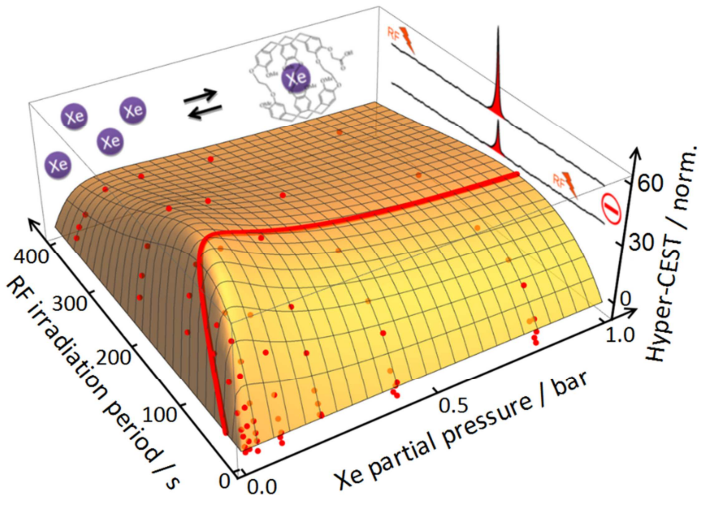

Figure 1: Model and measurement for 90 nM cryptophane-A mono acetic acid (CrAma) in aqueous solution at 298 K.[4] Hyperpolarized xenon binds reversibly to the CrAma (left upper part). The saturation of the magnetization of CrAma-bound xenon by RF irradiation leads to a diminished free hpXe signal when applied on resonance (right upper part). The difference to the signal intensity for RF applied off resonance is determined by Hyper-CEST and can be mapped in dependence of the saturation duration and the free xenon concentration (or xenon partial pressure for xenon saturated solution). Experimental data (red dots) are scaled with a global fit parameter and superimposed on the plot of the model function $S(\rho,\tau,\omega)$ evaluated for appropriate parameters and variables settings. Because of the slow exchange, the saturation efficiency is practically unity, rendering S independent from ω. Apparent is a distinguished maximum on the red crest line.

NMR of Reversibly Bound Xenon beyond Classic Hyper-CEST Detection: Displacement Assays and T_2 Exchange Effects

Leif Schröder
Molecular Imaging, Leibniz-Forschungsinstitut für Molekulare Pharmakologie (FMP), Berlin, Germany; lschroeder@fmp-berlin.de

Background: Reversibly bound xenon has been explored in chemical exchange saturation transfer (CEST) measurements for more than a decade[1] with great success in improving sensitivity for NMR and MRI of so-called functionalized ^{129}Xe. While the original detection scheme focuses on the transient residence of only Xe in the host molecules and relies solely on the detection of a selective knock-out of magnetization, recent studies include the interaction with competitive guests to alter the net saturation transfer and/or to cause an observable change in T_2 relaxation of unbound Xe.

Methods: The reversible binding of Xe with cucurbit[n]urils[2] was investigated in the presence of different competitive guests that also bind into a host cavity and cause displacement of Xe to various degree. This has an impact on the achievable CEST effect and the effective T_2 of free Xe.

Results: We could successfully follow the course of the enzymatic conversion of lysine into cadaverine by lysine decarboxylase[3] where the product has a strong affinity to the host cucurbit[6]uril (see Fig.1). Progress of the reaction causes a loss in CEST amplitude and an increase in T_2. Similarly, the binding of Aβ40 and α-synuclein cause a loss in the CEST effect from cucurbit[7]uril.

Conclusions: This talk will give an overview of recent projects in our lab that go beyond the classic Hyper-CEST detection scheme for sensing of different analytes and expanding the set of high-sensitivity tools for diagnostic purposes.

Sources of Funding: Koselleck SCHR 995/5-1 Grant by the German Research Foundation (DFG) and grant no. 12549 by The Michael J. Fox Foundation for Parkinson's Research.

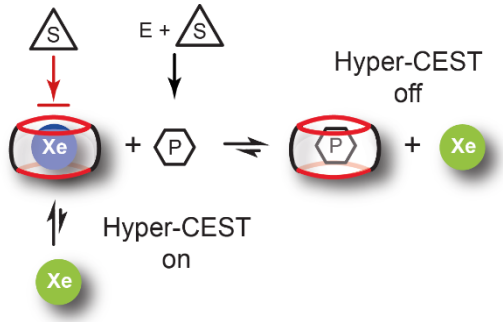

Fig. 1: Competitive binding of an enzymatic product (P) on the one hand and of ^{129}Xe on the other hand to a supramolecular host is used for detecting a gradual loss in the Hyper-CEST response. It enables to monitor the initial reaction rate for conversion of the substrate (S) and to derive the specific activity of the enzyme (E) .

References:

(1) Schroder, L.; Lowery, T. J.; Hilty, C.; Wemmer, D. E.; Pines, A. Molecular Imaging Using a Targeted Magnetic Resonance Hyperpolarized Biosensor. *Science* **2006**, *314* (5798), 446–449.
(2) Kunth, M.; Witte, C.; Hennig, A.; Schröder, L. Identification, Classification, and Signal Amplification Capabilities of High-Turnover Gas Binding Hosts in Ultra-Sensitive NMR. *Chem. Sci.* **2015**, *6* (11), 6069–6075.
(3) Döpfert, J.; Schnurr, M.; Kunth, M.; Rose, H. M.; Hennig, A.; Schröder, L. Time-Resolved Monitoring of Enzyme Activity with Ultrafast Hyper-CEST Spectroscopy. *Magn. Reson. Chem.* in print (2018).

Optical Pumping Laser with Picometer Linewidth and Stability

F. William Hersman[1,2], Jan Distelbrink[2], J. Ketel[2]
1. University of New Hampshire, Durham, NH 03824
2. Xemed LLC, 16 Strafford Avenue, Durham, NH 03824
Bill.Hersman@unh.edu

Background: While diode bar lasers are highly efficient for producing light in the near-infrared wavelength region, their spectral linewidth of several nanometers is two to three orders of magnitude too broad to be efficiently absorbed on alkali vapors in gaseous mixtures at pressures near one atmosphere. Linewidths can by reduced and concentrated around the desired wavelength by feedback from a diffractive element, either a volume bragg grating placed directly in front of the element or a planar grating in Littrow configuration at the focus of an afocal telescope. However, locating and maintaining the desired wavelength, especially for the narrowest linewidths, leads to increasing complexity and cost.
Methods: We report a new class of optical pumping laser that achieves wavelength stability and spectral narrowing by feedback through an atomic line filter. Optical polarization states have different indexes of refraction when passing through atomic vapor in a magnetic field. The Faraday effect rotates the orientation of plane polarization for longitudinal fields, while Voigt rotation occurs in transverse fields. Placing crossed polarizers at the entrance and exit creates an atomic line filter: it blocks all wavelengths that are not rotated, allowing only light that is in the midst of the resonance line (several hundred MHz in vacuum) to pass through. We assembled and characterized optical pumping lasers stabilized by atomic line filters using both Faraday and Voight rotation, using in-line and power-split architecture, with isotopically separated and natural rubidium vapor cells, and with diode laser bars at 795nm and 780nm. Beam splitters sampled light emitted from the diode, light passing through to the output, and light deflected by the polarizer. Spectra were analyzed with an Ocean-Optics spectrograph and one-meter Czerny-Turner monochromator. Efficiency was determined by integrating light in the line and comparing with light in the spectral shoulders. A production-ready prototype was tested by removing the afocal telescope and planar grating from a recently developed 3kW pump laser and replacing it with a high-power atomic line filter.
Results: The width of the output line was consistent with the 7pm linewidth of our Czerny-Turner monochromator. A shoulder on the lineshape indicates possible participation of lines filtered by Rb-85 and Rb-87, requiring further investigation (Fig 1). Narrowing efficiency was between 70% and 72% for both 780nm and 795nm, and for both Faraday and Voight rotation (although the latter required different optimal operating temperature and magnetic field.)

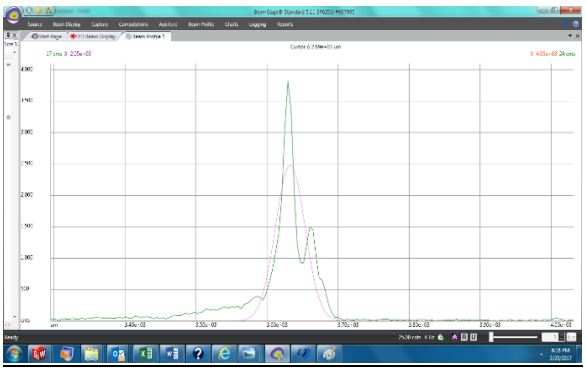

Fig. 1: FWHM equals the 7pm linewidth of our Czerny-Turner monochromator.

Conclusions: An optical pumping laser wavelength-stabilized by feedback from an atomic line filter provides high efficiency, absolute wavelength stability and ultra-narrow linewidth, ideal for optical pumping alkali vapors in gas mixtures at low and modest pressures.
Funding source: Internal research and development fund, Xemed LLC

Synthesis of Novel Macromolecular and Supramolecular Hosts for Binding Xenon

Brenton DeBoef,[a] Ashvin Fernando,[a] Paul Cesana,[a] Brianna Peloquin,[a] Scott Karas,[a] Francis T. Hane,[b] Braedan R. J. Prete,[b] Yurii Shepelytskyi,[b] Tao Li,[b] Mitchell S. Albert[b]

[a] Department of Chemistry, University of Rhode Island, 140 Flagg Road, Kingston, RI 02881

[b] Thunder Bay Regional Research Institute, 980 Oliver Rd, Thunder Bay ON P7B 5E1

Presenting/corresponding author: bdeboef@uri.edu

Background. Like all molecular probes, hyperpolarized xenon-129 magnetic resonance imaging (HP-Xe MRI) biosensors consist of two functional parts, a binding component and a detection component that are joined by a covalent tether. The binding component is usually a small molecule, peptide or antibody that binds to a specific analyte or biochemical receptor, allowing for the detection and characterization of specific biochemical phenomena. The detection component for a HP Xe biosensor is usually a supramolecular cage-like structure that can encapsulate a xenon atom.[1] A relatively small set of xenon-binding molecules have been studied for their ability to bind the noble gas,[2] with the vast majority of work focusing on cryptophane and cucurbituril structures. Unfortunately, targeted molecular probes containing either of these xenon hosts are difficult to synthesize and/or functionalize. This presentation will describe our efforts to design and synthesize novel macrocyclic and supramolecular architectures for their ability to bind xenon in aqueous environments.

Methods. Host compounds containing cavities of sufficient size and hydrophobicity for binding xenon atoms were modeled using the commercial computational chemistry packages Spartan 16 (Wavefunction, Inc.) and Molecular Operating Environment (Chemical Computing Group). The hosts were then synthesized by standard organic methods, and characterized by NMR, mass spectroscopy and isothermal calorimetry. Hyperpolarized xenon-129 chemical exchange saturation transfer (HyperCEST) experiments were performed at 3T in a clinical MRI scanner using a home-built fritted phantom and a custom dual-tuned $^{1}H/^{129}Xe$ coil.

Results. We have recently synthesized and studied three new molecular scaffolds that can be detected by HyperCEST: benzene-substituted CB6, pseudorotaxanes, and pillararenes. Importantly, the pseudorotaxanes and pillararenes that we have designed are water soluble, can be easily synthesized in multi-gram quantities, and can be functionalized by Diels-Alder or substitution reactions.

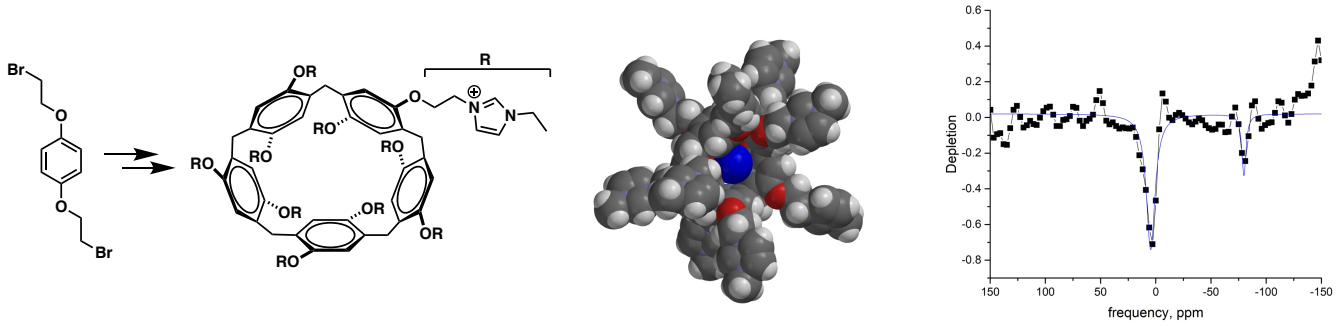

Figure. Two-step synthesis of a water-soluble pillararene (left), computational model of the pillararene binding a xenon atom (center), and HyperCEST data that confirming the reversible binding (right).

Sources of Funding. The DeBoef lab is supported by a grant from the Rhode Island Research Alliance, and the Albert lab is supported by a Natural Sciences and Engineering Research Council (NSERC) Discovery grant.

References

(1) Schröder, L. Xenon for NMR Biosensing--Inert but Alert. *Phys Med* **2013**, *29*, 3–16.

(2) Wang, Y.; Dmochowski, I. J. An Expanded Palette of Xenon-129 NMR Biosensors. *Acc. Chem. Res.* **2016**, *49*, 2179–2187.

Advances in Hyperpolarized Xenon-129 Magnetic Resonance Imaging

Mitchell Albert, Ph.D.[1,2,3], albertmi@tbh.net*; Francis Hane, Ph.D.[1, 2], Tao Li, MSc.[1]*

(1) Department of Chemistry, Lakehead University, Thunder Bay, ON, Canada. (2) Thunder Bay Regional Health Research Institute, Thunder Bay, ON. Canada. (3) Northern Ontario School of Medicine, Thunder Bay, ON, Canada.

The field of hyperpolarized xenon-129 magnetic resonance imaging (HP ^{129}Xe MRI) has grown immensely since its inception, providing a unique imaging method for the brain, lungs, and body. In 1994, Dr. Mitchell Albert and colleagues invented this imaging technology (1) and since then, lung applications have been widely studied using helium-3 and xenon-129 (^{129}Xe). The field is now expanding to include brain and molecular imaging using HP ^{129}Xe.

HP ^{129}Xe MRI is uniquely beneficial for brain imaging due to the ability of ^{129}Xe to cross the blood-brain barrier. In addition, as a foreign element in the human body, ^{129}Xe MRI does not suffer from background signals from other tissues, such as muscle and blood. This imaging modality has been used for the measurement of cortical brain function and stroke models in animals where the signal voids can be observed in the ischemic core (2-4). Recently, the Albert group has successfully shown the novel use of HP ^{129}Xe MRI as an agent for functional brain MRI, in which the signal enhancement is greater than with conventional proton blood-oxygen-level dependent (BOLD) functional MRI (5). In addition, HP ^{129}Xe MRI has been used to study cerebral perfusion of xenon in participants with Alzheimer's disease compared to healthy controls. Preliminary results have shown a slower washout time in grey and white matter for Alzheimer's disease participants compared to healthy controls (Figure 1)(6). Dr. Albert's research group is excited about the potential use of HP ^{129}Xe MRI for early detection of Alzheimer's disease biomarkers.

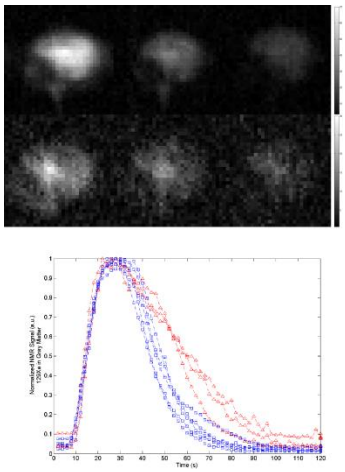

Figure 1. (a) Representative sagittal ^{129}Xe dynamic images from the brain of a healthy participant (top) and an AD participant (bottom). **(b)** Wash-in and wash-out time course of ^{129}Xe signal in grey matter from both healthy (blue) and AD participants (red).

Molecular imaging using HP ^{129}Xe MRI is another sub-field that has emerged from hyperpolarized gas MRI. HP ^{129}Xe molecules can be detected with high sensitivity using MRI and thus, there is potential to attach these molecules to cage molecules that will bind to disease specific biomarkers in the body. Building on the work of Schroeder et al., Dr. Albert's group obtained the first *in vivo* images of a xenon biosensor, cucurbit[6]uril (CB6), using the hyperpolarized Chemical Exchange Saturation Transfer (hyperCEST) effect to image the vascular system of a living animal model (7, 8). The hyperCEST effect results in amplification of the depleted solvent pool and leads to a signal enhancement that is up to a billion times greater than thermally polarized xenon (7). The CB6 cage molecule is non-functionalized but can be used with the hyperCEST technique and HP ^{129}Xe as proof of principle that there is potential to detect disease biomarkers with HP ^{129}Xe MRI. Current work is focused on the synthesis of functionalized CB6 molecules, and a scaffold molecule of benzCB6 has already shown potential as it is able to demonstrate a hyperCEST effect.

References

(1) Albert MS, Cates GD, Driehuys B, Happer W, Saam B, Springer Jr. CS & Wishnia A. Nature. 1994;370:199-201. **(2)** Rao et al. Proc. Intl. Soc. Mag. Reson. Med. 24 (2016), 0722. **(3)** Zhou et al. NMR Biomed 2010 24:170–175. **(4)** Mazzanti et al. PLoS One 2011 6:e21607. **(5)** Hane et al. Proc. Intl. Soc. Mag. Reson. Med. 25 (2017), 4745. **(6)** Li et al. Proc. Intl. Soc. Mag. Reson. Med. 25 (2017), 487. **(7)** Schroeder L et al. Science. 2006; 314: 446-440.**(8)** Hane et al. Scientific Reports 7, 41027 (2017), doi:10.1038/srep41027.

Xenon (and other gas) Complexation: From Cages with Chemical Shift Modifiers to Porous Molecular Solids

K. Travis Holman
Department of Chemistry, Georgetown University, 37th and O St. NW, Washington, DC 20057
kth7@georgetown.edu

Background, Methods, Results, Conclusions. Xenon is an expensive gas due to its broad utility—lighting, lasers, ^{129}Xe NMR probes, silicon etching (as XeF_2), anesthesia, spacecraft propellant, *etc.*—and its low concentration in the atmosphere (87 ppb), requiring production via energy-intensive cryogenic distillation of large volumes of air. The development of materials for the selective inclusion/sorption/binding of xenon/krypton is a growing area of research driven by the potential for transformative rare gas production, separation, storage, and/or recovery technologies. Similarly, the development of discrete molecules with high affinity for xenon in solution is driven by emerging applications in low detection limit sensing based upon hyperpolarized ^{129}Xe NMR spectroscopy/imaging. This talk will focus on our development of new discrete molecules and molecule-derived materials for the selective complexation, sorption, and/or storage of gases, and particularly xenon, for various applications. New cage-like molecular platforms relevant to ^{129}Xe NMR sensing technologies will be discussed,[1] along with concomitant efforts in studying the materials properties of various new xenon/gas clathrates and gas-sorbing materials.[2-4]

Source(s) of Funding. National Science Foundation (DMR-1610882)

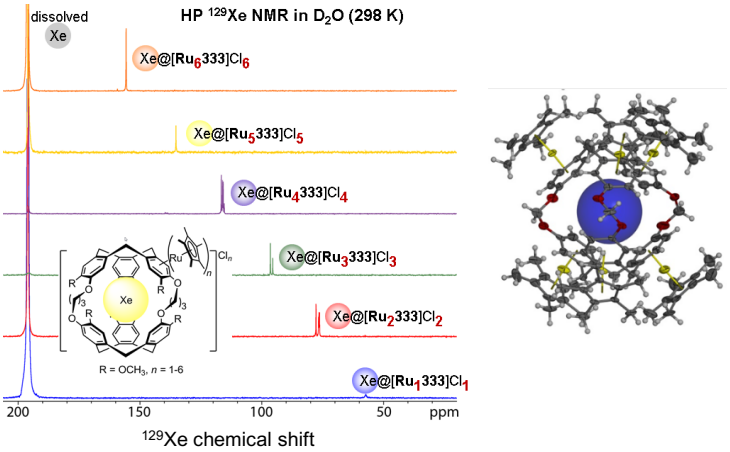

Figure 1. (left) Hyperpolarized ^{129}Xe NMR spectra (298 K, D_2O) of several Xe@[**Ru$_x$**(cryptophane-**333**)]Cl_x (x = 1-6) species exhibiting the electron withdrawing effect of the organometallic moieties. The multiple peaks for x = 2-4 are due to the compounds being regioisomeric mixtures. (data credit: Berthault *et al.*) (right) Crystal structure of the Xe@[**Ru$_6$**(cryptophane-111)]$^{6+}$ complex (chloride counter ions omitted).

References.

1. El-Ayle, G.; Holman, K. T. "Cryptophanes," In *Comprehensive Supramolecular Chemistry II*; Atwood, J.L., Gokel, G. W., Barbour, L. J., Eds.; Elsevier: New York, **2017**; Vol. 6, 199-249.
2. Kane, C. M.; Banisafar, A.; Dougherty, T. P.; Barbour, L. J.; Holman, K. T. *J. Am. Chem. Soc.* **2016**, *138*, 4377–4392.
3. Joseph, A. I.; Lapidus, S. H.; Kane, C. M.; Holman, K. T. *Angew. Chem. Int. Ed.* **2015**, *54*, 1471–1475.
4. Joseph, A. I.; El-Ayle, G.; Boutin, C.; Léonce, E.; Berthault, P.; Holman, K. T. *Chem. Commun.* **2014**, *50*, 15905-15908.

Quantitative Hyperpolarized ^{129}Xe Imaging in the Free-breathing Mouse

Stephen Kadlecek, Kai Ruppert, Luis Loza, Mehrdad Pourfathi, Sarmad Siddiqi and Rahim Rizi
University of Pennsylvania Department of Radiology (stephen.kadlecek@uphs.upenn.edu)

Background: Like hyperpolarized ^{3}He, ^{129}Xe is used to visualize lung ventilation and gas redistribution/diffusion. However, its blood/tissue solubility and phase-specific chemical shift also allow visualization of gas uptake into tissue and blood, and flow into the heart, vasculature and more distal locations. We present images acquired in a free-breathing mouse that highlight and quantify these processes. Although there are significant signal-to-noise and resolution challenges posed by short T2* in fields typically associated with mouse imaging, slow gas delivery and extended averaging is used to achieve images of high quality. Quantification is achieved by comparing images acquired in steady state using different RF pulses; these images differ in a way that is determined by uptake, delivery or replacement rates, thereby allowing determination of organ function in specific circumstances.

Methods: Images were acquired in BAL/b mice using a Bruker 9.4T Avance spectrometer with gradient insert. During imaging, animals breathed freely from a flowing mixture of 20ml/min HP ^{129}Xe (40-50%, Xemed Xebox) mixed with 100 ml/min O_2-enriched air to maintain FiO2 near 0.2. Four types of images were acquired: High-resolution gas-phase (ventilation) images, Dissolved phase Ultra-short Echo Time (UTE) images utilizing varying repetition times and flip-angles on a 128x128 grid (402 radial spokes), Chemical Shift (CSI) images acquired on a 64 x 36 oversampled grid (4096 FIDs) with varying flip-angles, and quantitative gas phase specific ventilation images using breath-triggered gradient-echo imaging at flip-angles of 10-90 degrees. Along with the dissolved phase images, low flip-angle gas phase image were acquired simultaneously or interleaved with the dissolved image for intensity normalization. Image sets acquired with different relaxivities (flip-angles or TRs) were fit to a model of signal buildup and decay to quantify specific ventilation or dissolved gas uptake and delivery times.

Results: The figure shows a set of images exemplifying: a) (blue box) a high-resolution gas phase image in a post-transplant lung, showing the anastomosis of the left bronchus and the lobar fissure, b) (green box) breath-triggered gas phase images acquired using flip-angles of, from left to right, 15, 30, 60 and 90 degrees. The higher flip-angle images accentuate rapidly-exchanging gas, and modeling of this process yields the fractional ventilation map at the right. c) (black box) a proton image showing a tumor in the left lung, along with the accompanying d) CSI dissolved-phase images acquired with flip-angles of 10, 20, 40, 70 and 90 degrees. Note that in this case lower flip-angles (shown to the right) accentuate later arrival times for the dissolved gas, allowing visualization of, in order, the lung parenchyma, left atrium, left ventricle, aortic arch and descending aorta, kidneys, and finally vena cava and fat deposits. This progression is summarized in the arrival time map (s) at the right.

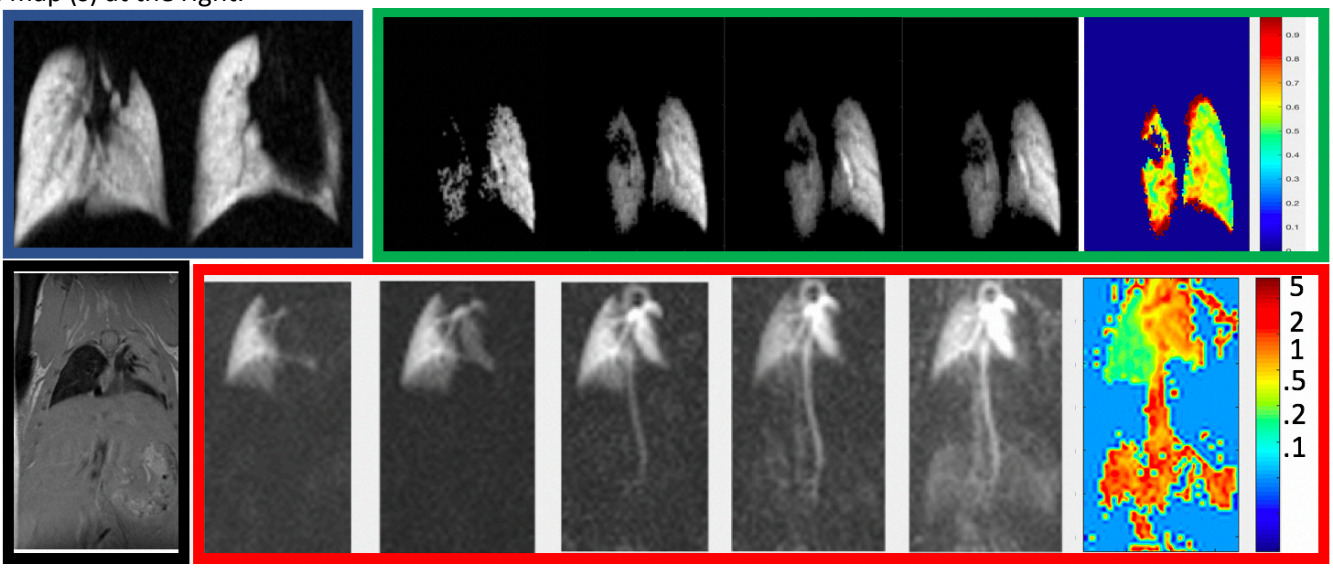

Conclusions: Although high-resolution mouse imaging using hyperpolarized ^{129}Xe is challenging, the rapid breathing and low gas delivery rates can be used advantageously in conjunction with variation of the acquisition parameters to locally quantify a variety of ventilation and gas uptake parameters that are known to be modified in disease. In particular, the dissolved phase images highlight the ability of xenon to mimic the uptake and delivery of oxygen throughout the body of the mouse. This sensitivity to the entire range of lung function is difficult to achieve using any other technique.

References: 1) Iguchi, et al., Magn Reson Med 70(1):207-215 (2013). **Research Support:** NIH R01 HL139066

Hyperpolarized ^{129}Xe Lung MRI and Biosensors @ China

Xin Zhou

State Key Laboratory of Magnetic Resonance and Atomic and Molecular Physics, National Center for Magnetic Resonance in Wuhan, Wuhan Institute of Physics and Mathematics, Chinese Academy of Sciences, Wuhan, 430071, P. R. China.

Computed tomography (CT) is a popular and routine imaging modality to evaluate lung diseases, and has shown a substantial value for clinics. However, the use of CT in longitudinal studies is limited because of exposure to ionizing radiation. Magnetic resonance imaging (MRI) does not use ionizing radiation and therefore can be used repeatedly in longitudinal studies. Unfortunately, MRI of the lung airways is not possible due to the exceedingly low density of nuclear spins present in the air space.

With the technique of spin-exchange optical pumping (SEOP), the spin polarization of hyperpolarized xenon can be enhanced four or five orders of magnitude, which makes feasible to obtain the gas phase signal, like in the lung's airspace morphology. We built a new designed ^{129}Xe hyperpolarizer with a two-body optical cell, which can produce hyperpolarized ^{129}Xe with ~20% polarization for natural abundance xenon[1-2]. It enables us to image lung with hyperpolarized natural abundance xenon, showing a great potential for applying in clinics. By using hyperpolarized ^{129}Xe ADC or ADK MRI, the microstructure of smoke-induced lung can be well visualized and evaluated [3-4]. Being a trace element in the atmosphere, xenon is soluble in water, blood and tissues. Therefore, dissolved phase xenon MRI could provide rich information related to the gas-exchange function of the lung. The morphological and physiological parameters of the radiation-induced lung injury (RILI), chronic obstructive pulmonary diseases (COPD) and emphysema can be non-radioactively and non-invasively obtained in vivo using hyperpolarized ^{129}Xe diffusion, CSSR and CEST MRI [5-8], which could not be achieved by the currently imaging modalities. It demonstrates that such a new imaging technology is able to evaluate the microstructure and function of the lung, which paves a new way for the pulmonary disease research. Furthermore, different xenon biosensors were designed and developed to specifically detect ions, biothiols and H_2S in living cell [9-13], showing the potential great applications of hyperpolarized xenon MRI in biomedicine.

References

1. Deng H, et. al, Zhou X. ***J. Magn. Reson.*** 263: 92–100 (2016).
2. Zhong J, et. al, Zhou X. ***Sci. Rep.*** 6, 25854. (2016).
3. Ruan W, et. al, Zhou X. ***J. Magn. Reson. Imag.*** 45(3), 879-888. (2017)
4. Ruan W, et.al, Zhou X. ***Magn. Reson. Med.*** 78(5), 1891-1899. (2017).
5. Li H, et. al, Zhou X. ***Magn. Reson. Med.*** 76: 408-416 (2016).
6. Deng H, et. al, Zhou X. ***Sci. Rep.*** 6, 35760. (2016).
7. Zhang Z, et. al, Zhou X. ***Biomed. Phys. Eng. Express***, 2: 055013 (2016).
8. Zhong J, et. al, Zhou X. ***NMR Biomed.*** 30(8), e3730 (2017).
9. Guo Q, et. al, Zhou X. ***Chem. Eur. J.*** 22: 3967-3970 (2016).
10. Yang S, et. al, Zhou X. ***Anal. Chem.*** 88: 5835-5840 (2016).
11. Li H, et. al, Zhou X. ***NMR Biomed.*** 29: 220-225 (2016).
12. Zeng Q, et. al, Zhou X. ***Anal. Chem.*** 89, 2288 (2017).
13. Yang S, et. al, Zhou X. ***Chem. Eur. J.*** 23,7648 (2017).

Acknowledgements

This work was supported by the National Natural Science Foundation of China (81227902, 81625011) and National Program for Support of Eminent Professionals (National Program for Support of Top-notch Young Professionals).

Hyperpolarized liquid ^{129}Xe for ultralight dark matter detection

John W. Blanchard, for the CASPEr Collaboration
Helmholtz-Institut Mainz
blanchard@uni-mainz.de

The nature of dark matter is one of the most important open problems in modern physics. Axions (originally introduced to resolve the strong CP problem), or axion-like particles (ALPs) are strongly motivated dark matter candidates, but are difficult to detect experimentally. The Cosmic Axion Spin Precession Experiment (CASPEr) [1] uses NMR techniques to detect spin precession induced by ultralight (sub-μeV) axion/ALP dark matter.

The essence of CASPEr is straightforward: under appropriate experimental conditions, ALPs induce spin precession when interacting with nuclear spins [2]. In one version of the experiment (CASPEr-Wind), nuclear spins couple directly to the relative velocity of the ALP field such that one can treat the ALP-nuclear spin coupling as a pseudo-magnetic field, $\boldsymbol{B}_{ALP}\,(t)$ with amplitude proportional to the coupling strength, direction given by the electric field or relative velocity, and oscillation frequency determined by the ALP mass. As shown schematically in Fig. 1, it is thus possible to search for ALP dark matter using a field-swept CW-NMR experiment where the RF driving field $\boldsymbol{B}_1$ is replaced with $\boldsymbol{B}_{ALP}$; when the nuclear Larmor frequency is equal to the ALP frequency, $\boldsymbol{B}_{ALP}$ drives nuclear spin precession into the transverse plane, such that the oscillating magnetization can be measured using an appropriate sensor.

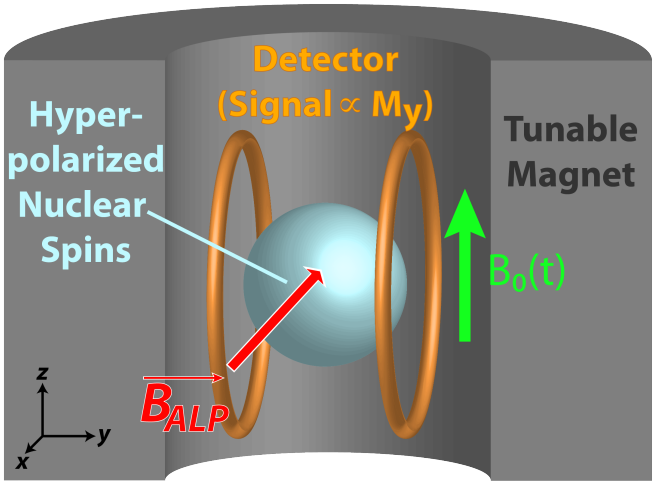

Figure 1. *Cartoon-level schematic of the CASPEr concept. A sample consisting of polarized nuclear spins is acted upon by the ALP-induced effective magnetic field,* $\boldsymbol{B}_{ALP}$*. A tunable superconducting magnet produces a time-dependent field* B_0 *such that when the nuclear Larmor frequency is equal to the frequency of the ALP field, the nuclear spins will precess into the XY plane, resulting in measurable transverse magnetization.*

The first-generation experiment will use superconducting quantum interference devices (SQUIDs) to measure any flux generated by the transverse magnetization of an 8-mm diameter sphere of liquid ^{129}Xe spin-polarized via spin-exchange optical pumping (SEOP). We will sweep the magnetic field from $\pm 10^{-4} - 10^{-1}$ T, which corresponds to ^{129}Xe Larmor frequencies from ~1 kHz to ~1 MHz, or axion/ALP masses from about $5\times10^{-12} - 5\times10^{-9}$ eV. I will describe the current state of the experiment, with an emphasis on the Xe polarization, purification, and liquification stages.

[1] D. Budker, et al. Proposal for a Cosmic Axion Spin Precession Experiment (CASPEr). *Phys. Rev. X* **4**, 021030 (2014).
[2] P.W. Graham, S. Rajendran. New observables for direct detection of axion dark matter. *Phys. Rev. D* **88**, 035023 (2013).

Ultrafast Laplace NMR with hyperpolarized xenon

O. Mankinen[1], J. Hollenbach[2], S. Ahola[1], J. Matysik[2] and V.-V. Telkki[1]
[a] NMR Research Unit, Faculty of Science, University of Oulu, Oulu, Finland.
[b] Institut für Analytische Chemie, Universität Leipzig, Leipzig, Germany.
E-mail: otto.mankinen@oulu.fi

NMR relaxation and diffusion measurements provide detailed information about dynamics and structures of substances such as porous materials, and reveal interactions of nuclei with their microscopic environment. Since relaxation and diffusion data comprise exponentially decaying components, the processing requires a Laplace inversion in order to extract the diffusion coefficient and relaxation time distributions. Thus, these methods are referred to as Laplace NMR (LNMR). [1]

Multidimensional approach increases the chemical resolution of an NMR experiment, but, at the same time it makes the experiment time much longer as compared to one dimensional counterparts. The increased experiment time prevents one to follow fast processes (e.g. protein folding). In ultrafast Laplace NMR [2-4] single-scan experiments become feasible by means of spatial encoding of two-dimensional data, similarly to ultrafast NMR spectroscopy introduced by Frydman et al. [5]. The price to pay is slightly reduced sensitivity. However, single-scan approach enables the use of hyperpolarization methods (e.g. PHIP, DNP [3] and SEOP [4]), which provide much higher sensitivity boost than the loss due to spatial encoding.

In this presentation we introduce the concept and recent progress of multidimensional ultrafast LNMR. We demonstrate that, applying spatial encoding and hyperpolarization of xenon, we are able to decrease the experimental time by many orders of magnitude and, at the same time, increase the sensitivity of the experiment significantly. The ultrafast LNMR method also allows us to investigate dynamics of gases absorbed in porous structures which is not possible with ultrafast NMR spectroscopy. The ultrafast LNMR methods are applicable by mobile NMR instruments, thus widening the application range even further [6].

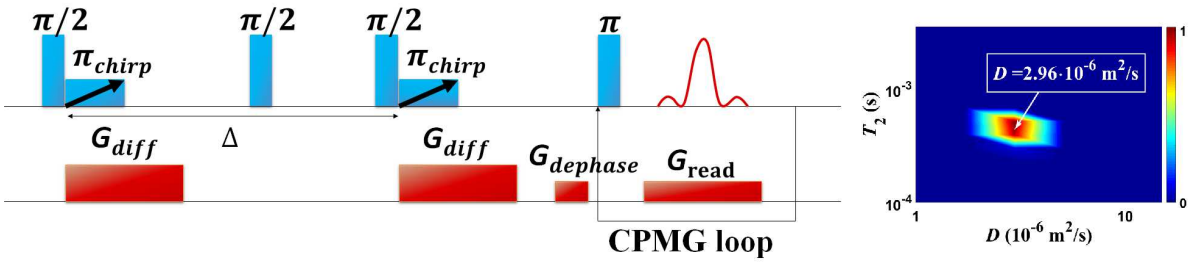

Figure 1: Left: The pulse sequence of ultrafast D-T_2 -correlation experiment. Right: D-T_2 correlation map of free hyperpolarized xenon.

[1] Y. Q. Song, *J. Magn. Reson.* **229**, 12-24, 2013.
[2] S. Ahola, V.-V. Telkki, *ChemPhysChem*. **15**, 1687-1692, 2014.
[3] S. Ahola, V.V. Zhivonitko, O. Mankinen, G. Zhang, A.M. Kantola, H.-Y. Chen, C. Hilty, I.V. Koptyug, V.-V. Telkki. *Nat. Commun.* **6**, 8363, 2015.
[4] O. Mankinen, J. Hollenbach, S. Ahola, J. Matysik and V.-V. Telkki, *Microporous Mesoporous Mater. In Press, (2017) DOI:10.1016/j.micromeso*.2017.10.024
[5] A. Tal and L. Frydman, *Prog. Nucl. Mag. Res. Sp* **57**, 241–292, 2010.
[6] J.N. King, V.J. Lee, S. Ahola, V.-V. Telkki, and T. Meldrum, *Angew. Chem. Int. Ed.*, **55**, 5040-5043, 2016.

The financial support of Academy of Finland (grants #289649 and #294027), University of Oulu Graduate School, Tauno Tönning Foundation, Orion research Foundation and KAUTE foundation is gratefully appreciated.
.

In situ high pressure ^{129}Xe NMR spectroscopy of pressure-amplifying flexible Metal-Organic Frameworks (MOFs)

Felicitas Kolbe[1], Simon Krause[2], Irena Senkovska[2], Stefan Kaskel[2], Eike Brunner[1]

[1] Chair of Bioanalytical Chemistry, Department of Chemistry and Food Chemistry, TU Dresden, 01062 Dresden, Germany (contact: felicitas.kolbe@tu-dresden.de)

[2] Chair of Inorganic Chemistry I, Department of Chemistry and Food Chemistry, TU Dresden, 01062 Dresden, Germany

In DUT-49 (Dresden University of Technology No. 49), a mesoporous metal-organic framework, and related materials (DUT-47, DUT-48, DUT-50), adsorption-induced structural transitions lead to adsorption phenomena such as negative gas adsorption.[1] *In situ* experiments are especially powerful to study the host-guest interactions responsible for transitions in these materials.[2] ^{129}Xe NMR experiments were carried out using a homemade *in situ* apparatus which allows high-pressure NMR spectroscopic studies at variable gas pressures up to saturation. By observing the chemical shift at different pressures, we obtain adsorption/desorption isotherms. It is also possible to study the gas exchange by 2D EXSY experiments.

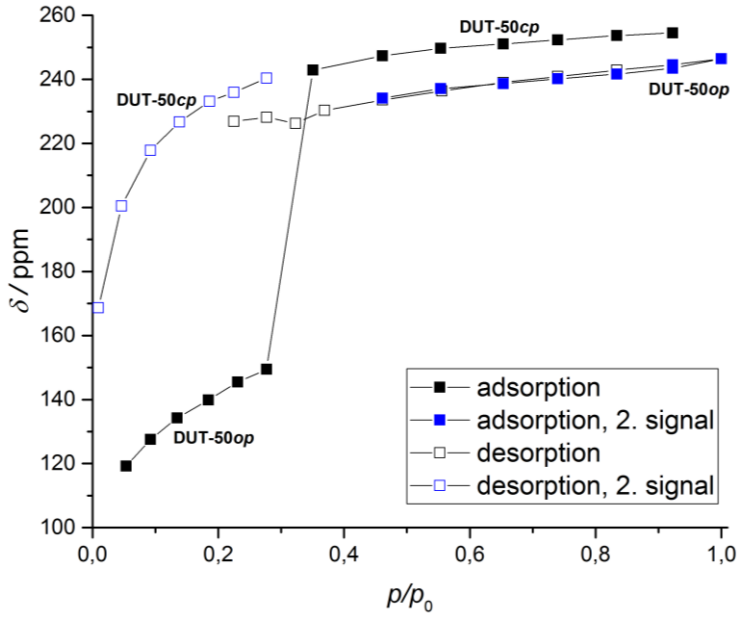

Fig. 1: Chemical shifts of adsorbed xenon in DUT-50 at 200 K measured during the adsorption experiment.

At the beginning of the adsorption experiment the pores of mesoporous DUT-50 are open. A sudden shift jump from 149 ppm to 243 ppm at $p/p_0 = 0.3$ indicates a structural contraction to DUT-50*cp* (contracted pore). This is even accompanied by desorption at increasing pressure (negative gas adsorption[1]). At a temperature- and adsorbent-dependent gate-opening pressure DUT-50 switches from the *cp* back to the *op* (open pore) state and a second signal for xenon adsorbed in DUT-50*op* appears (Fig. 1). A change from *op* to *cp* state can be observed upon desorption. Even at lower pressures, DUT-50 stays at this conformation. Accordingly, DUT-50 is the second known material besides DUT-49, which shows the phenomenon of negative gas adsorption during the adsorption process.

Funding source: Financial support by the DFG (FOR 2433 MOF Switches) is gratefully acknowledged.

(1) Krause, S. *et al. Nature* **2016**, *532* (7599), 348–352.

(2) Schaber, J. *et al. J. Phys. Chem. C* **2017**, *121*, 5195–5200.

Flow, dispersion, and relaxation studies in chemical reactors with hp ^{129}Xe.

Thomas Meersmann

Sir Peter Mansfield Imaging Centre, University of Nottingham,
Nottingham, NG7 2RD, United Kingdom.
Thomas.Meersmann@Nottingham.ac.uk

Background: Many industrial applications involve gas flow and permeation in porous solids, such as catalytic reactors. The efficiency of heat and mass transfer in such systems impacts on the activity of the catalyst and the productivity of the process. The pressure and temperature in these systems is often such that gas density is low and diffusion is within the Knudsen regime (i.e. diffusion in heterogenous media with pore dimensions that are comparable or smaller than the mean free path of the diffusing particles). Hyperpolarization of xenon permits both structural and mass transport imaging, in particular for the study of low density and slow-moving gas transport in the Knudsen-regime that cannot be followed using other techniques.
Methods: Gas-phase hp ^{129}Xe MRI was used for velocimetry maps and dispersion maps where obtained through transport weighted MRI by varying the recycle delay under flow conditions. NMR spectroscopy was used to measure hp ^{129}Xe relaxation under stopped flow conditions. ^{1}H and ^{2}D T1 relaxation was measured using standard inversion recovery.
Results: Heterogeneity in mass transport in a packed bed of commercial, alumina, catalyst supports was obtained through stopped-flow hp ^{129}Xe MRI [1]. Significantly larger spatial variability in mass transport rates across the packed bed (over length-scales much larger than ~100 microns) was found compared to techniques using only molecular diffusion.
Using hp ^{129}Xe velocimetry, gaseous exchange was studied in channels with porous walls thus creating transverse permeability discontinuity in the otherwise Darcy flow. We have localized gas flow through channels in minilith-type pellets and the permeation of gas into their porous walls. The impact of the gas permeation into the porous wall can be detected indirectly through deviations in the channel flow profile from Poiseuille flow, due to a lack of the no-slip boundary condition, and from direct imaging of permeating gas within the porous walls themselves. The results where compared to pore-scale lattice Boltzmann modelling (LBM) of axially symmetric flow in a clear channel bound to a saturated porous medium to our experimental velocity fields [2].
The methodology was also applied to establish the structure-transport relationship in particulate filter that consist of hierarchical porous solids with ordered and disordered levels in the hierarchy. Hp gas phase MRI velocimetry allows to identify regions with dominant contribution to mass transport. Additional insights where obtained from the spin-lattice relaxation measurements with hyperpolarised ^{129}Xe to probe the changing free pore volume at various water saturation levels that affect mass transport as observed in the ^{129}Xe MRI dispersion maps. Three main step changes in T_1 at free pore volume fractions where found during drying of the materials caused by the porous hierarchy and the data correlates well with complementary ^{1}H and ^{2}D relaxation measurements.
Conclusions: Hp ^{129}Xe MRI can monitor mass transport in the Knudsen regime within reactors and filters. The technique provides information of chemical engineering related aspects of the porous hierarchy.
Funding: Engineering and Physical Sciences Research Council (EPSRC).

[1] Galina Pavlovskaya, et. al., 'NMR Imaging of Low Pressure, Gas-Phase Transport in Packed Beds Using Hyperpolarized Xenon-129', *AIChE Journal*, **61**, (2015), 4013 – 4019.
[2] Galina Pavlovskaya, et. al., 'Fluid flow in a porous medium with transverse permeability discontinuity', under review.